

Review

Advances in Amine-Surface Functionalization of Inorganic Adsorbents for Water Treatment and Antimicrobial Activities: A Review

Nabil Bouazizi * , Julien Vieillard , Brahim Samir  and Franck Le Derf

The Normandie Universite, UNIROUEN, INSA Rouen, CNRS, COBRA (UMR 6014), 27000 Evreux, France; julien.vieillard@univ-rouen.fr (J.V.); brahim.samir@univ-rouen.fr (B.S.); franck.lederf@univ-rouen.fr (F.L.D.)

* Correspondence: bouazizi.nabil@hotmail.fr

Abstract: In the last decade, adsorption has exhibited promising and effective outcomes as a treatment technique for wastewater contaminated with many types of pollutants such as heavy metals, dyes, pharmaceuticals, and bacteria. To achieve such effectiveness, a number of potential adsorbents have been synthesized and applied for water remediation and antimicrobial activities. Among these inorganic adsorbents (INAD), activated carbon, silica, metal oxide, metal nanoparticles, metal–organic fibers, and graphene oxide have been evaluated. In recent years, significant efforts have been made in the development of highly efficient adsorbent materials for gas and liquid phases. For gas capture and water decontamination, the most popular and known functionalization strategy is the chemical grafting of amine, due to its low cost, ecofriendliness, and effectiveness. In this context, various amines such as 3-aminopropyltriethoxysilane (APTES), diethanolamine (DEA), dendrimer-based polyamidoamine (PAMAM), branched polyethyleneimine (PEI), and others are employed for the surface modification of INADs to constitute a large panel of resource and low-cost materials usable as an alternative to conventional treatments aimed at removing organic and inorganic pollutants and pathogenic bacteria. Amine-grafted INAD has long been considered as a promising approach for the adsorption of both inorganic and organic pollutants. The goal of this review is to provide an overview of surface modifications through amine grafting and their adsorption behavior under diverse conditions. Amine grafting strategies are investigated in terms of the effects of the solvent, temperature, and the concentration precursor. The literature survey presented in this work provides evidence of the significant potential of amine-grafted INAD to remove not only various contaminants separately from polluted water, but also to remove pollutant mixtures and bacteria.



Citation: Bouazizi, N.; Vieillard, J.; Samir, B.; Le Derf, F. Advances in Amine-Surface Functionalization of Inorganic Adsorbents for Water Treatment and Antimicrobial Activities: A Review. *Polymers* **2022**, *14*, 378. <https://doi.org/10.3390/polym14030378>

Academic Editor: Iole Venditti

Received: 25 December 2021

Accepted: 14 January 2022

Published: 19 January 2022

Publisher's Note: MDPI stays neutral with regard to jurisdictional claims in published maps and institutional affiliations.

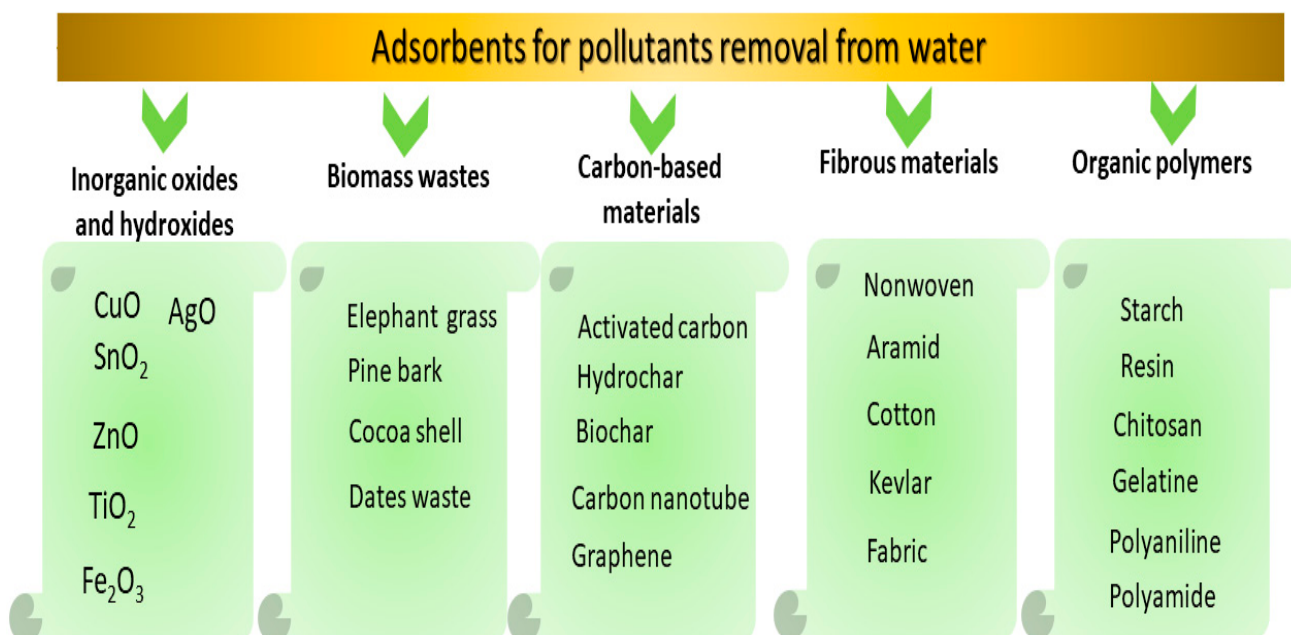


Copyright: © 2022 by the authors. Licensee MDPI, Basel, Switzerland. This article is an open access article distributed under the terms and conditions of the Creative Commons Attribution (CC BY) license (<https://creativecommons.org/licenses/by/4.0/>).

1. Introduction

The ever-increasing manufacturing industry and the huge range of resulting hazardous pollutants have considerably decreased the available amounts of drinking water [1–3]. This can have a dangerous effect not only on biological activities but also on human safety. For example, owing to incomplete use and washing operations, textile and other industries often discharge harmful dye effluents into water systems. Serious environmental pollution problems are caused by the high amount of heavy metals released in soil and water. In addition, the pharmaceutical industry widely discharges non-ecofriendly chemicals that may remain in spent water, which results in polluted effluents [4]. Toxic dyes in drinking water also pose a life threat to humans [5,6]. To solve these problems, several studies have focused on water treatment technologies [7–9]. Researchers recently focused on adsorption techniques to reduce water pollution [10–12]. Adsorption is commonly one of the best methods for reducing or removing hazardous pollutants and transforming them into safe inorganic compounds such as aminophenol [13–16]. In this context, many adsorbents

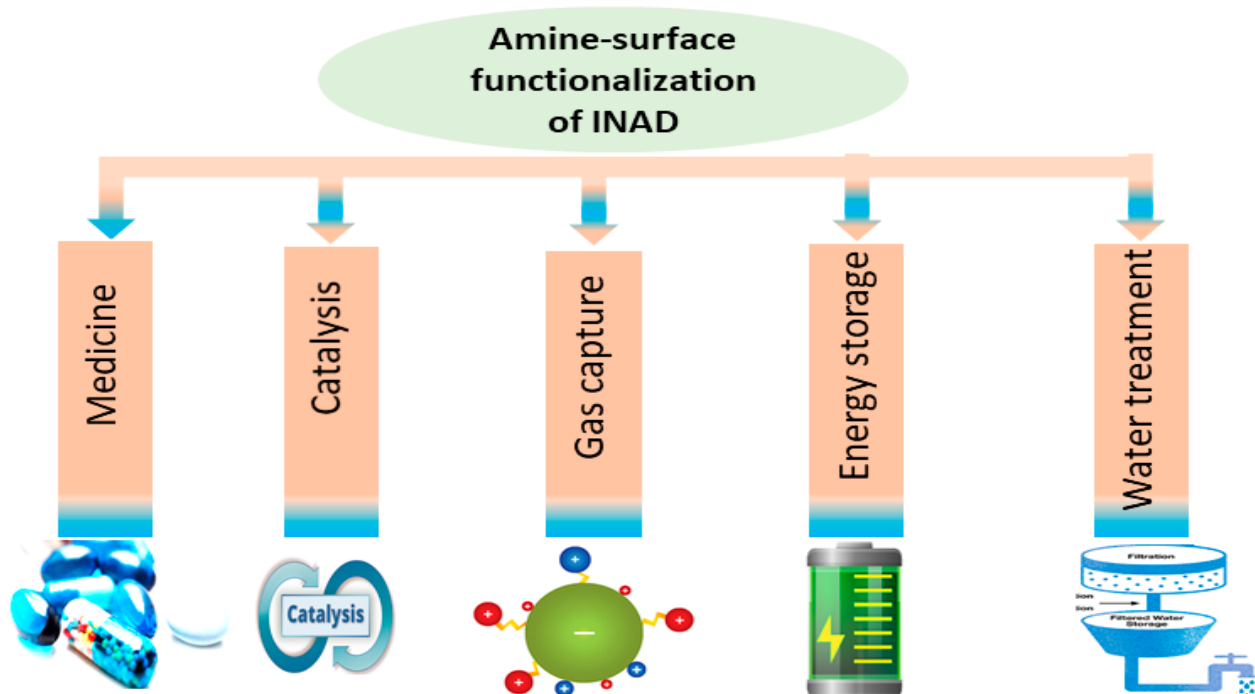
have been applied to adsorb contaminants from water, e.g., metal oxide nanoparticles (MO_x), activated carbon, biomass, graphene oxide, textile, polymers, clay, and many other sophisticated porous materials [7–16]. According to their main composition, the sophisticated porous materials can be classified as metal oxides/hydroxides, carbon-based materials, organic polymers, fibrous materials, and agricultural waste. Scheme 1 presents a view of the most effective and recently employed adsorbents for removing contaminants from liquid solution.



Scheme 1. Classification of adsorbents for pollutants removal from water.

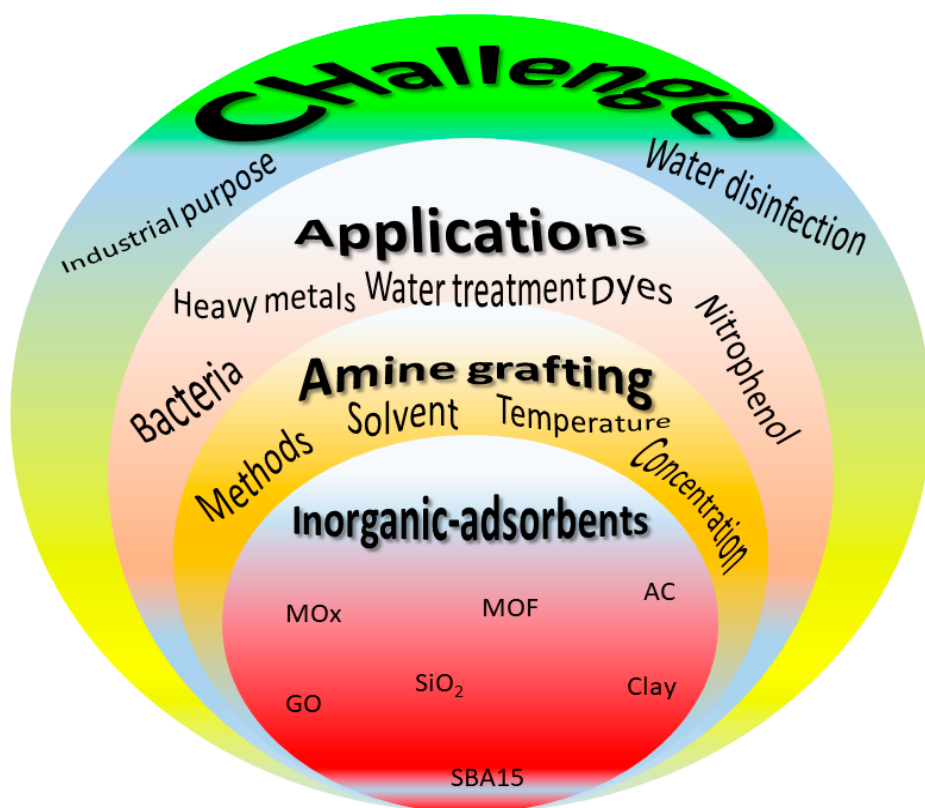
Despite the interesting properties and results on water treatment, the majority of these adsorbents showed a visible weakening in the continuous removal of toxic pollutants, poor reusability, and low adsorption capacity due to their surface properties. However, inorganic adsorbents (INADs) have attracted more interest in comparison to the other categories of adsorbents. This was explained by their surface properties and adsorptive characters: INADs lose their efficiency on water treatment because they are not stable enough. In this regard, techniques for surface modification and activation have been envisaged as effective pathways to enhance the separation and the effectiveness of INAD adsorbents [17–23]. Many works have been conducted to functionalize the porous materials and add more activated sites at the adsorbent surface. In order to improve the surface properties of these INADs, numerous organic molecules have been used to add new activated sites at the INAD surface [19–23]. Synthetic and natural organic compounds have demonstrated many advantages onto various materials, i.e., a simpler preparation technique, a lower cost, and effective strategies for the preparation of advanced composites. Among these organic molecules, amines are considered as the smart molecules with high values because they can increase both the adsorptive and antibacterial properties. Both natural and synthetic amines have a great effect on INAD stability and a great efficiency during environmental application. More particularly, 3-aminopropyltriethoxysilane (APTES), diethanolamine (DEA), dendrimer-based polyamidoamine PAMAM, and branched polyethyleneimine (PEI) are extensively employed for INAD functionalization and applications in microbiological and environmental catalysis, gas capture, and medical applications (Scheme 2) [17–23]. INAD functionalization via the chemical grafting of amines has increased the number of useful activated sites for adsorption and capture of toxic molecules. Metal oxides based on copper oxide (CuO), zinc oxide (ZnO), and tin oxide (SnO₂) modified via chemical grafting

of amines possess superior electrical, optical, catalytic, and antibacterial properties not attainable via their metallic alloy and monometallic counterparts [17,21,24–26].



Scheme 2. Amine and its multiple applications.

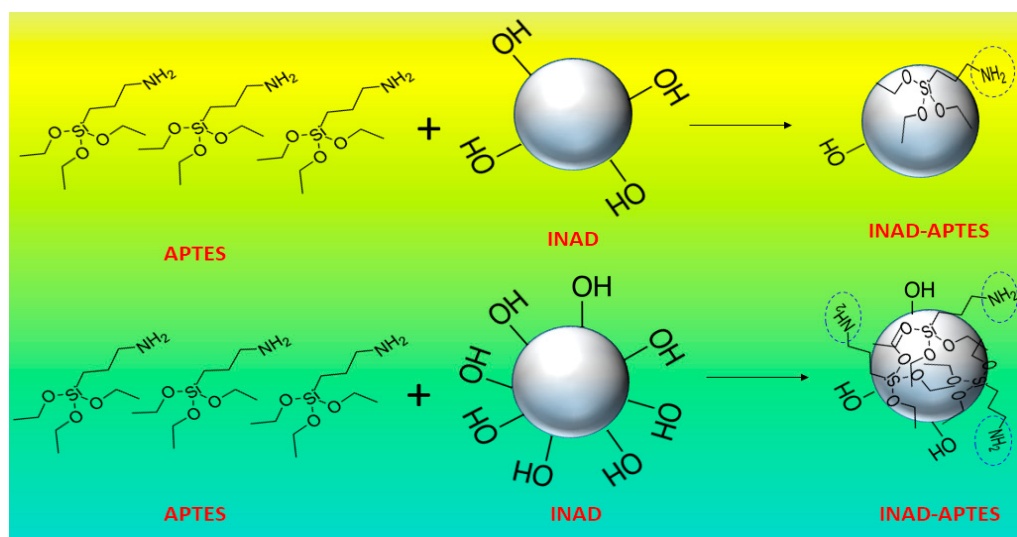
Chemical grafting of amine at the INAD surface occurs via a covalent interaction in which the molecules can persist for a long time. Covalent grafting of amine is one of the most sustainable and successful methods; it slightly decreases the surface area, while it increases the adsorption capacity. This method is regarded as a more efficient way of altering the specific properties of INAD and as a straightforward modification approach while significantly improving INAD properties. The existence of a positively charged amine group facilitates the attachment of many hazardous pollutants such as negatively charged bacterial cells, negative toxic molecules, and cationic and anionic dyes in liquid solution [27–32]. In other works, immobilized amine has been used to design and manufacture highly advanced materials such as 2D and 3D composites. Amine is employed as a link between the core and the shell for the synthesis of core–shell materials where amine plays a key role in the stabilization and sustainability properties of the resulting materials. The enhanced stability and surface compatibility of amine with porous materials can be achieved through the kinetic trapping of amines surrounding the porous materials. However, further efforts are still required to fully elucidate the intimate relationship between amine-modified INAD structures and their adsorption of wastewater pollutants and their antibacterial properties [19–32]. The goal of this review is to provide a view of the surface functionalization via grafting of amines and their adsorption behavior in water treatment. The strategies utilized for the grafting of amine at the INAD surface are established and compared in terms of concentration, temperature, and solvent. In addition, the reactions and interactions are investigated. The literature survey presented in this paper provides evidence of the good potential of amine-grafted INAD materials for removing several contaminants from aqueous solution through adsorption. The contents of this review are illustrated in Scheme 3.



Scheme 3. The general contents of the present review.

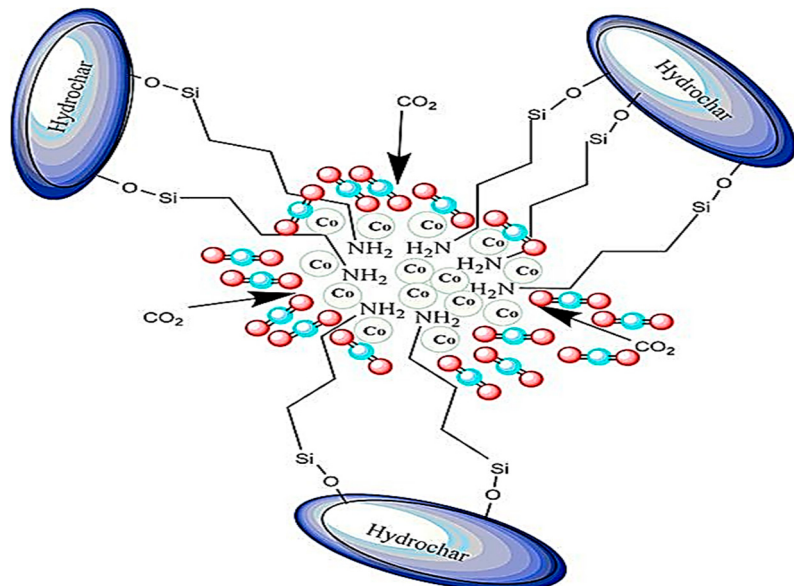
2. Amine for Surface Functionalization of Adsorbents

The surface properties of INAD play an important role on the extent of the interaction between adsorbents and adsorbates. Consequently, surface modification and functionalization have been targeted to improve the stability and adsorptive properties of porous materials for water treatment and to increase their adsorption capacity, as well as reducing toxicity. INAD adsorbents generally have a negatively charged surface coming from the hydroxyl groups ($-OH$) and saturated oxygens. As a result, INADs become unstable and their efficiency can be highly reduced. Consequently, in most cases, INADs lose their adsorptive properties. This can be explained by the competitive interaction between the negatively charged elements (i.e., the OH groups and unsaturated oxygen) and the adsorbates [18,33–35]. INAD based on metal-loaded biomass and hydrochar has been functionalized by APTES grafting to lower the number of OH groups present at the INAD surface. Hydroxyl groups have been found necessary for the grafting of high amounts of amine onto the INAD surface (Scheme 4). By comparing the adsorption capacity of an unmodified adsorbent with a negatively charged surface and its modified counterpart, it is clear that hydroxyl groups destabilize the materials involving a competition between adsorbents/adsorbate. The adsorption capacity of unmodified adsorbents is lower than that of their modified counterparts. Amine-modified adsorbents visibly increase the adsorption uptake of various toxic molecules and improve the reutilization of the materials, suggesting their high stability. Despite its low adsorption efficiency, it is important to note that negative surface charge can be advantageously used for subsequent surface modifications via covalent coupling using silane chemistry or via physical adsorption or electrostatic interactions.



Scheme 4. Schematic illustration of hydroxyl groups for APTES grafting onto a hydrochar surface.

Surface functionalization of INADs can be carried out by distinct strategies involving both chemical and physical interactions. For amine grafting, the relevant interactions likely involved during the reaction process are covalent interactions, hydrogen bonding, and electrostatic interactions. Most of these interactions enhance the surface properties, particularly surface activation and the adsorptive character. Covalent functionalization at the INAD surface based on silica is made possible by the well-established silane chemistry, which mediates strong linkages between the INAD surface and aminosilane. Despite being well established, silane chemistry can present drawbacks that result in steric hindrance and/or uneven reactivity depending on the coupling agents, and limitation to molecules with reactive groups for the covalent linking step. However, hydrogen bonding is widely used for adsorbing gas molecules, which is beneficial for the reversible reaction between gas release and adsorption. For example, the grafting of amine based on APTES at the metal-loaded biochar and metal oxide demonstrated that amine could involve interactions between the gas molecules and aminosilane via both hydrogen bonding and electrostatic interactions, as supported in Scheme 5.



Scheme 5. Electrostatic interactions between amines and gas molecules (CO₂). Reprinted from [35] with permission from Elsevier.

Until now, hydrogen bonding and electrostatic interactions have been the most commonly used strategies for the preparation and functionalization of adsorbents for reversible gas adsorption. However, amine grafting via covalent interactions has played a key role in the improvement of adsorptive properties and recyclability, particularly for wastewater treatment. Table 1 reports different amine-modified INAD adsorbents employed for removing various pollutants from water. Bouazizi et al. employed several types of amine such as APTES, PAMAM, DEA, and others for the surface functionalization of porous materials [18,20,22,24]. Results obtained in water treatment showed that covalent grafting of amine onto the adsorbent is of great interest to increase the adsorption uptake and the number of recycling cycles. Most of these amine molecules have been commonly used as stabilizing and coupling agents because they promote strong covalent linkages onto the INAD. For example, surface functionalization with PAMAM has been extensively used and is another example of such a type of surface modification. PAMAM with terminal NH₂ groups is a dendrimer with amine terminal groups that acts as a protective layer around the adsorbent surface in these situations. This method has quite often been used to attach microorganisms such as Gram+ and Gram– bacterial strains *Staphylococcus epidermidis* and *Escherichia coli* and organic pollutants (nitrophenols and dyes). Due to its opposite charges, PAMAM interacts with the surface of colloidal nanoparticles [18,19]. While these grafting methods are efficient for the adsorption application, the grafting strategies depend on the solvent, the concentration, and the temperature of the media.

Table 1. Summarized inorganic adsorbents (INADs) functionalized by amine grafting for environmental applications.

INAD	Amines	Potential Application	Reference
Coconut coir pith	Amine-modified polyacrylamide	Removal of Cr(VI)	[36]
Coconut coir pith	Amino-functionalized polyacrylamide	Removal of phosphate	[37]
Microspheres (Fe ₃ O ₄ @mesoporous SiO ₂ core–shell composite microspheres)	Polyethyleneimine	Adsorption of humic acid (HA) Removal of heavy metals	[38,39]
Kaolin composite	Acrylamide	Removal of cesium and cobalt	[40]
Montmorillonite	Quaternized poly vinylpyridinium-co-styrene	Removal of selenate, potassium arsenate, methyl blue, eosin-Y, atrazine, and sulfentrazone	[41]
Polymer clay	Starch with quaternary ammonium groups	Removal of pharmaceuticals	[42]
Montmorillonite	Quaternized poly vinylpyridinium-co-styrene	Removal of the anionic pharmaceutical diclofenac (DCF)	[43]
Clay (heulandite)	Chitosan	Removal of Cu(II) and As(V)	[44]
Chitosan/PVA/PES	Fe ₃ O ₄ -NH ₂	Removal of Cr(VI)	[45]
Magnetic graphene composite	1,2-ethylenediamine	Removal of Cr(VI), Pb(II), Hg(II), Cd(II), and Ni(II)	[46]
Fe ₃ O ₄	1,6-hexanediamine	Removal of Cr(VI) and Ni(II) ions	[47]
Magnesium ferrite nanoparticles (MgFe ₂ O ₄)	Mesoporous amine NH ₂	Removal of Pb(II)	[48]
Fe ₃ O ₄ /NaP zeolite nanocomposite	3-aminopropyltrimethoxysilane	Removal of Pb(II), Cd(II), and bacteria	[49]
Magnetic illite–smectite clay	3-aminopropyltriethoxysilane	Adsorption of Pb(II) ions	[50]
Magnetite nanocomposites	Chitosan nanoparticles and polythiophene	Removal of Hg(II)	[51]

Table 1. *Cont.*

INAD	Amines	Potential Application	Reference
Core–shell magnetic nanoparticles	3-aminopropyltriethoxysilane and nitrilotriacetic acid	Removal of Cu(II) and Sb(III)	[52]
Chitosan-coated magnetite	Hydrazinyl amine	Removal of Ni(II) and Pb(II)	[53]
Maghemite nanoparticles	Glycine	Removal of Cu(II)	[54]
Magnetic nanoparticles	Diocetylphthalate triethylenetetraamine	Removal of Zn ions	[55]
Magnetic nanoparticles $\text{Fe}_3\text{O}_4@\text{SiO}_2$	3-aminopropyltriethoxysilane	Removal of Zn(II) ions	[56]
Bentonite/ $\text{CoFe}_2\text{O}_4@\text{MnO}_2$ magnetite	3-aminopropyltriethoxysilane	Removal of Cd^{2+}	[57]
Activated carbon, derived from waste rubber tires	Diethylenetriamine	Removal of phenol	[58]
Magnetic bamboo-based activated carbon	Ethylenediamine	Removal of ciprofloxacin and norfloxacin	[59]
Cocoa shell	Aminosilane	Reversible CO_2 capture	[35]
Graphene oxide	3-aminopropyltriethoxysilane	Reduction in 4-nitrophenol	[23]
Copper oxide (CuO) nanosheets	P-aminothiophenol and diethanolamine	Potential uses in catalysis and biomedical applications	[21]
Polyester fabrics (PET)	3-aminopropyl triethoxysilane	Degradation of 4-nitrophenol (4-NP) and methylene blue	[60]
Cocoa shell	3-aminopropyltriethoxysilane	Removal of chromate and nitrate	
Cocoa shell	3-aminopropyltriethoxysilane	Desorption of CO_2	[34]
Activated carbon	pentaethylenehexamine	Removal of lanthanum	[61]

3. Effect of the Solvent

The solvent is an essential parameter for the grafting of amines at the surface of INADs, and can have a great influence on the effectiveness of the reaction and the rate of grafted amines (Table 2). The solvent affects the surface and the wetting properties of the material, and this favors the control of the grafting process at the surface or the inner material. Researchers recently studied the functionalization of mineral-clay-based INADs by using 3-aminopropyltriethoxysilane (APTES) in the presence of various solvents such as distilled water, tetrahydrofuran, toluene, and ethylene glycol. The solvents with a low surface energy wetted the adsorbent easily and thereby made it possible for silane to interact with the -OH groups present at the INAD surface. However, the wetting process was lower for the solvents with a higher surface energy for water, and this relatively decreased surface adsorption. In other works, ethylene glycol was used as a solvent for chemical grafting of amines which indicated a low amount of aminosilane incorporated onto the INAD [62]. When organic solvents such as cyclohexane and toluene are used as anhydrous products, the evaluation of amine grafting at the INAD surface takes a long time (20 h) for the 3-aminopropyltetraethoxysilane using the reflux method [63]. The obtained adsorbent shows a visible change of the structure materials, with an expanded or distorted molecular structure (Table 2). In summary, the presence of water facilitates the initial hydrolysis of amines on the INAD surface, depending on the volume of water [64,65]. Results of the degradation of toxic pollutants by various INADs reported in literature show that APTES grafting has a superior adsorption capacity of toxic molecules in the presence of $\text{H}_2\text{O}/\text{amine}$ as compared with the anhydrous or hydrated solvent. In detail, when water is absent from the synthesis protocol, amines bind directly to the hydroxyl group at the surface of the INAD. However, excess water in the medium promotes the polymerization of amines during the functionalization process.

The nature of the dispersant medium has been pointed out too: protic solvents are not favorable to the grafting process because of potential competition reactions. A competitive interaction is indeed involved between the alkyl siloxane and hydroxyl groups of the solvent, and it allows H-bonding rather than hydroxyl group bonding. Aprotic solvent has been used to enhance favorable solvent–surface interactions [66,67]. To explain the mechanism occurring during the grafting onto silica-based INAD, the following steps are the main reactions involved in the process. Firstly, amine enters a hydrogen bonding interaction: the hydroxyl groups at the surface or the basic amine function inter-react with a proton from a hydroxyl group and produce an ionic bond. Due to the last type of interaction, which is more stable than the first one, the hydrogen-bonded molecules self-catalyze the condensation on the silicon side of the silane molecule, and a covalent bond is formed. Upon condensation on the silicon side, the amine group loses its interaction with the surface and the amine points away from the surface. The higher number of ethoxy groups on the APTES molecule leads to a much faster stabilization. Thus, the aminosilane molecule turns from the original amine-down position to an amine-up position.

Table 2. Summary of the solvent, temperature, and grafting methods of various amines.

Amine Precursors	Solvents	Temperature (°C)	Grafting Strategies	Reference
APTES	Water	Room temperature	Conventional synthesis	[66]
APTES	Toluene	45; 120	Reflux	[65,68]
APTES	N,N-Dimethylformamide	175	Microwave-assisted synthesis	[68]
APTES	Water–ethanol mixture (25:75 vol.)	80	Conventional heating, reflux	[69]
APTES	Cyclohexane	60	Reflux	[70]
DEA	Ethanol	70	Reflux	[71]
DEA	Sodium carbonate solution	80	Conventional heating	[72]
2-AEAPS	Hexane	(not mentioned)	Reflux	[73]
PAMAM	Hydroalcohol	70	Conventional heating	[18]
HMD	Water–ethanol mixture (25:75 vol.)	80	Conventional heating	[26]
DAN	Hydroalcohol	80	Conventional heating	[74]
APTMS	Toluene/water	85	Reflux	[75]
DETA	Epoxy Chloropropane/dimethylformamide	95	Conventional heating	[76]
ATP	Dichloromethane	0	Conventional cooling	[77]
TEA	Trimethylamine	Room temperature	Conventional synthesis	[78]

4. Effect of Temperature

An increase or decrease in the synthesis temperature can influence the resulting products, but also play a crucial role in the amine grafting at the INAD surface. Various synthesis temperatures have been used for grafting amines onto INAD (Table 2). In most cases, the temperature rise is typically going along with an increase in the interactions between the amine molecules and the surface hydroxyl groups. Xue et al. [65,79] studied the role of temperature on the grafting of APTES in the presence of toluene as a solvent for a series of temperatures (15 °C, 30 °C, 45 °C, 60 °C, and 75 °C). The results showed that chemical grafting of APTES was promoted by increased temperature. Bouazizi et al. and Bertuoli [17,35,80] investigated the grafting of APTES at the INAD surface in ethanol/water (75:25, v/v) at 50 °C and 80 °C. The temperature increase allowed for a high interaction of the amine groups with the adsorbent. High temperature (220 °C) was also found to be the favorite pathway for the diffusion of amines onto the adsorbent [81]. Based on the above findings, elevating the concentration of amines such as 3-aminopropylphosphonic acid

(3APPA) or 3-propylphosphonic acid (3PPA) and high temperature results in an increased modification degree.

5. Effect of the Concentration

In order to ensure effective grafting of amines at the INAD surface, the amine concentration plays a crucial role in the preparation of advanced functional adsorbent materials. Considering the weight of amines, high amounts of amine can affect the properties of the support used for post treatment. On the one hand, increases in the amine concentration can mean that more active terminal groups such as $-\text{NH}_2$ have interacted with the adsorbent surface via $-\text{OH}$ groups. In this way, the high amount of amine can increase the terminal target of the functional groups on INAD as a support. Xue et al. [65] investigated the grafting of aminosilane with different ratios, and the results showed an improvement of the adsorption capacity for dye removal when the ratio is increased. On the other hand, in this context, the adsorption uptake decreased slightly when the amine concentration increased. The high number of amine molecules that surrounded the INAD surface affected its porosity and decreased its adsorption capacity. The enhancement of the adsorption uptake can be explained by the incorporation of high numbers of amines onto the INAD surface. Until now, no explanation has been found as to why the adsorption capacity of INAD decreases when the concentration of the precursors increases. In other works, a large molecular weight of amines improved the stability of the adsorbent [82,83]. PEI functionalized with 1,2-epoxybutane (EB) was synthesized by Choi et al. [83]. The proportion of primary amine gradually decreased, while the proportion of secondary amine and tertiary amine gradually increased. Consequently, the grafting of 1,2-epoxybutane onto INAD improved the stability and the adsorptive properties. More recently, they also demonstrated that increases in the molecular weight of amines induced superior thermal stability. The resulting material had O/N molar ratios of 0.42, 0.64, and 0.82, respectively, as shown in Figure 1.

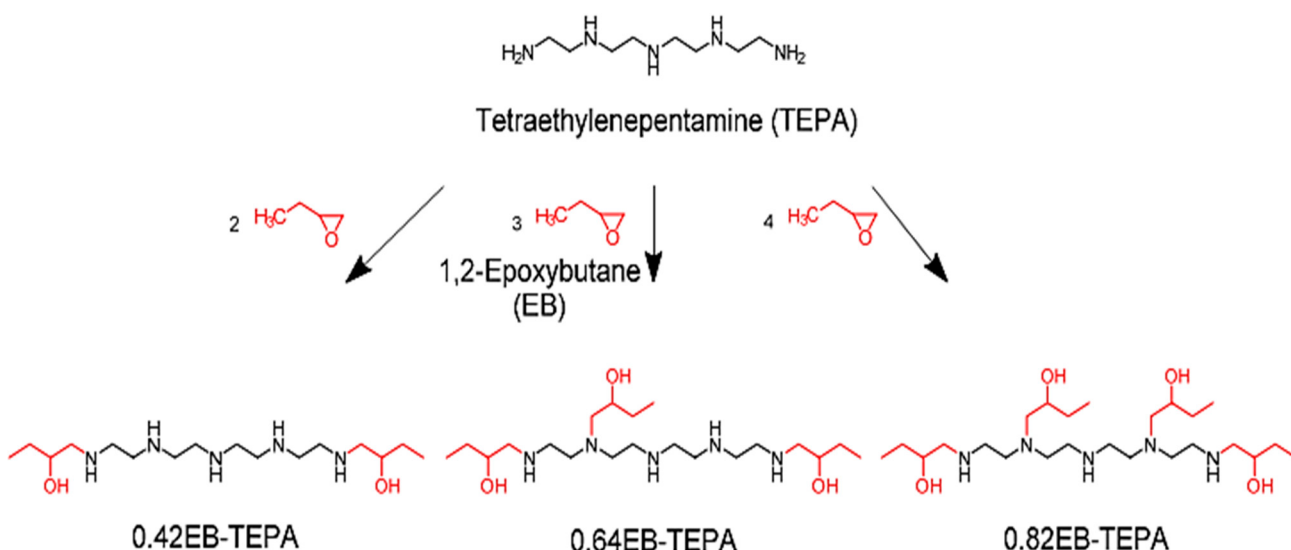


Figure 1. Functionalization of TEPA using different amounts of EB. Reprinted from [84] with permission from the American Chemical Society.

6. Influence of Amines on the Hydrophilic Characters

The grafting of amines can influence the hydrophilicity and hydrophobicity of INADs. In order to investigate the effect of amine immobilization, contact angle measurements were employed to study wettability, surface energy, and diffusion resistance. Bouazizi et al. investigated the hydrophilic properties of INADs modified with amines such as DEA, PAMAM, and aminosilane. The contact angle results showed that the INAD surface became more hydrophilic than the original one. Amine intercalation in the adsorbents increased their hydrophilic character, and this improved diffusion or the transfer rate of organic

molecules from the aqueous solution toward the INAD surface [18]. In addition, amine grafting introduced a visible decay of the hydrophilic surface, evidenced by the loss of the OH stretching bond [19]. This behavior was also recorded for DEA(OH)₂ grafting, which decreased the hydrophilic character, given the consecutive decrease until total loss of the hydroxyl groups. Therefore, we can conclude that amine grafting increases the hydrophilic character as it decreases the number of hydroxyl groups present at the adsorbent surface. In another work, amine grafting induced a visible decrease in the hydrophilic character in relation to slight compaction of the structure. This can be explained by hydrophobic interactions within the aminosilane entanglement and strong interactions between amino and surrounding -OH groups. In this regard, these interactions imply that diffusion is hindered, causing slow initial wettability without affecting the hydrophilic character. On the contrary, metal–organic frameworks (MOF) functionalized by inserting 2-aminoterephthalic acid showed an increase in the hydrophobic character of the adsorbent [77]. The surface morphology of both unmodified and amine-modified MOF remained unchanged, but their hydrophilic properties decreased, as supported in Figure 2.

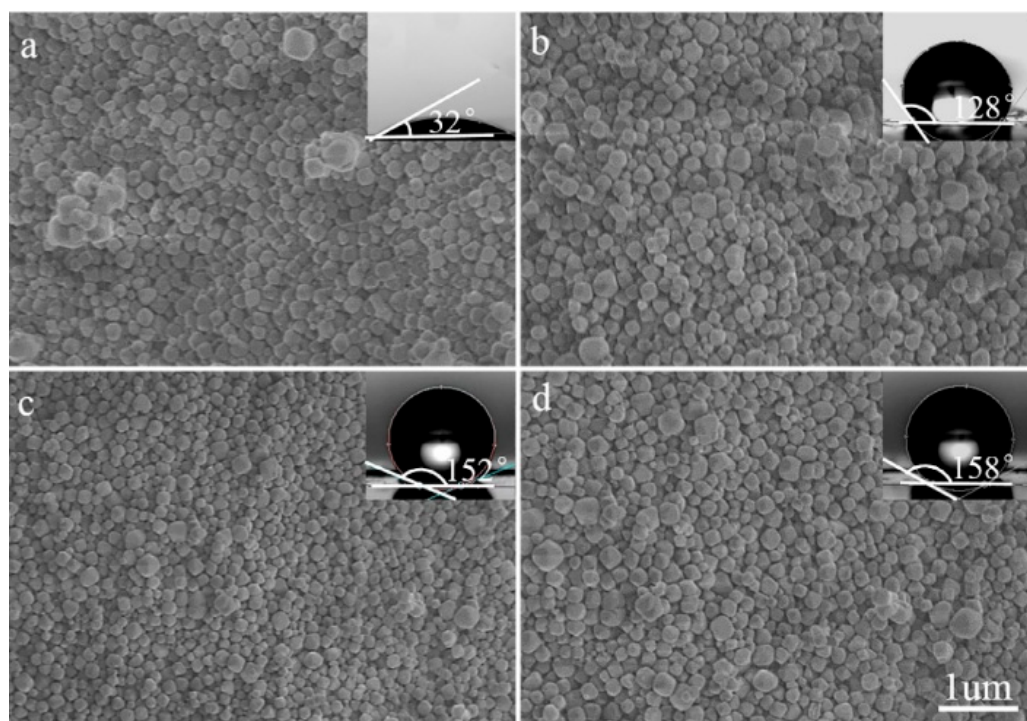


Figure 2. SEM images of (a) untreated MOF and (b–d) amine-functionalized MOF prepared with various concentrations of precursor. Inserts are photographs of water droplets used to determine the hydrophilic character. Reprinted from [77] with permission from Elsevier.

It was recently demonstrated that the contact angle increased as the number of amine groups decreased. While the quantity of amines rose from 0.1 vol.% to 10 vol.%, the contact angle increased, suggesting a higher coverage of the INAD surface. This last result is of great interest for wastewater treatment because it shows that amine molecules can interact with the adsorbent surface in a well-organized manner to maximize their adsorptive properties. Again, the hydrophilic characteristics of amine-modified adsorbents are explained by the remaining hydroxyl groups that lower the contact angle. Consequently, the obtained hydrophilic charters are very helpful for removing pollutants from water.

7. Chemical State of the Amine Groups

FTIR and XPS analysis were employed to investigate the presence of the different chemical states of the amine groups and the surface compatibilities attributed to those states. The band observed at 1582 cm^{-1} was associated to the bending vibration of NH_2 , which is visible as a shoulder on the deformation mode of molecular adsorbed water (Figure 3) [85,86]. The broad band between 1540 and 1490 cm^{-1} was associated to the asymmetric deformation vibration of the NH_3^+ groups [87–90]. In addition, the position of the NH_2 band shifted toward the lower wavenumbers as compared with those recorded for the aqueous solutions of primary amines. This was explained by the presence of hydrogen bonding interactions with NH_2 groups [91]. In this case, the nitrogen atom (N) is considered as a hydrogen acceptor [87]. The same trend was obtained by Bouazizi et al., where a similar shift (from 1600 to about 1575 cm^{-1}) was recorded for APTES grafted with metal oxide and activated carbon [23]. These results evidence an interaction between amine and silanol groups, which result in a variety of hydrogen-bonded surface conformations such as an intramolecular membered ring structure. Another confirmation was obtained by the presence of hydroxyl groups ($\text{Ti}-\text{OH}$) available for hydrogen bonding and or acid/base interactions. Additionally, amine grafting onto INAD induced distortion of the surface chemistry resulting in structure expansion in some cases and structure compaction in others.

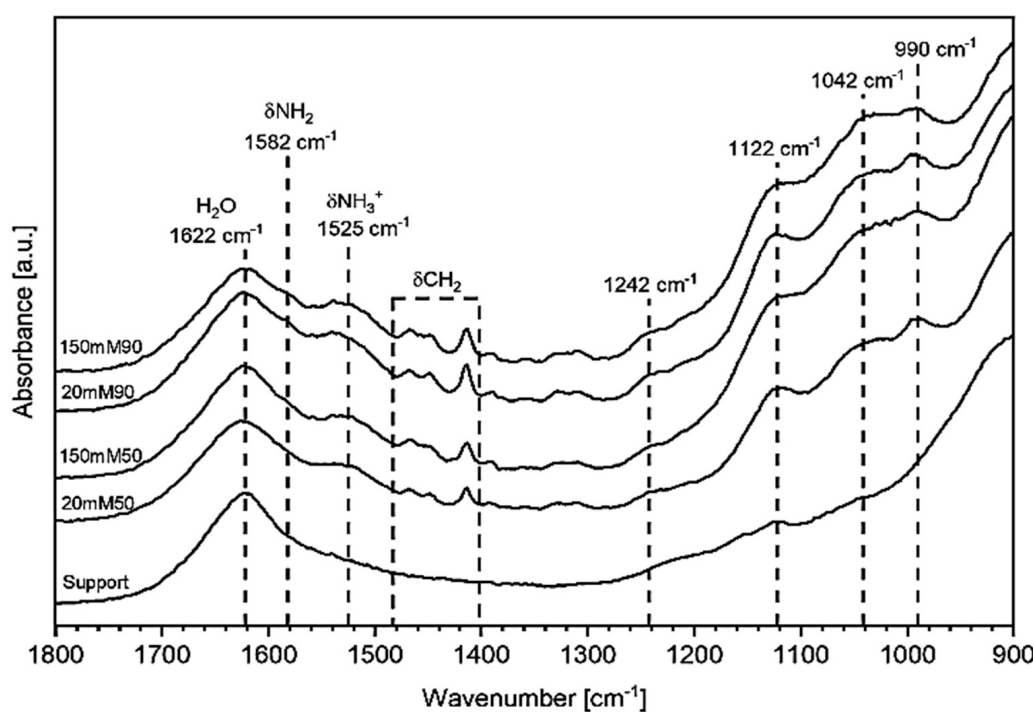


Figure 3. Infrared spectra of 3APPA grafted with mesoporous TiO_2 samples, at the lowest (20 mM) and highest concentrations (150 mM) for two different temperatures: $90\text{ }^\circ\text{C}$ and $50\text{ }^\circ\text{C}$. Reprinted from [92] with permission from Elsevier.

XPS analysis provided data about the amine molecules through high-resolution observation of N1s. The peak observed at 399.8 eV was attributed to the traces of molecularly adsorbed N_2 . However, upon amine addition, the N1s peak of amine-loaded INAD consisted of a broad asymmetric peak composed of two bands at 398 and 400 eV (Figure 4). Until now, it has been hard to draw a conclusion about these peaks, as N1s data showed various types of interactions that can have a similar binding energy, which are considered as complicating factors [93–95]. The peaks at low binding energy (398 eV) can be associated to the non-interacting NH_2 groups or to Lewis acid-base interactions. Consequently, the component at high binding energy at 401 eV is associated to protonated amine (NH_3^+) groups originating from proton transfer from $-\text{OH}$ groups. The hydrogen-bonded amine

groups are hard to observe experimentally by XPS. Although other peaks' position and ratio of NH_2 and NH_3^+ for INAD evidenced that amines addition occurred with specific surface arrangements. [92]. Basically, the above results prove that possible surface conformations of amines such as 3APPA at the INAD surface can be established via the free NH_2 groups accessible for interactions with their surroundings. In other cases, the NH_2 groups can involve intra- and inter-adsorbate interactions and adsorbate–surface interactions, with 3APPA amine as the adsorbate [95].

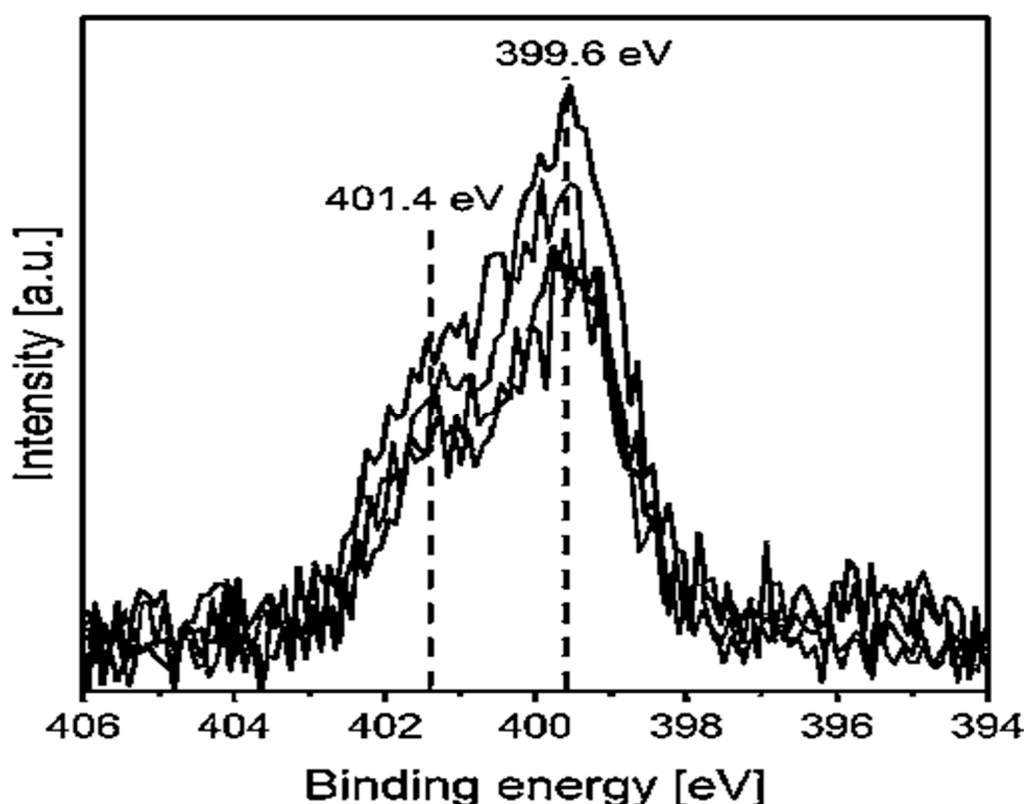
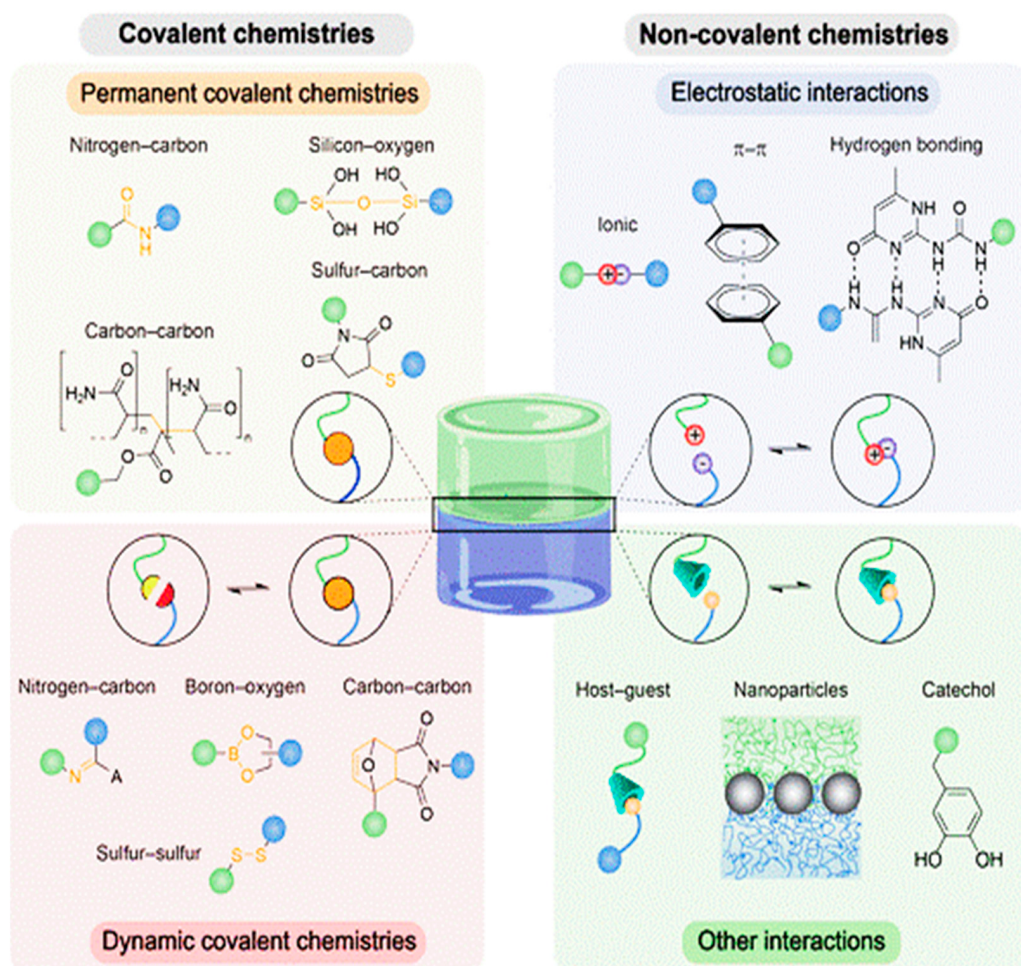


Figure 4. N1s spectra of 3APPA samples grafted with TiO_2 . Reprinted from [92] with permission from Elsevier.

Recent research has been conducted in the field of amine utilization for biomedical applications. Amines have proved very useful for an effective junction and design of high-value biomedical INADs [96]. In this case, amines play a key role to elaborate a biomedical hydrogel in 2D and 3D shapes. In this case, amines allow for the formation of links or connections between other chemicals at the surface to ensure the creation of surface compatibility. Amines can adhere to and design the surface materials via several interaction types and relate bond chemistry to the emergent adhesive properties with a specific emphasis on biomedical applications (Scheme 6).



Scheme 6. Illustration of the amine bond chemistries that can be employed as adhesion junctions in the preparation of materials. Adhesion junctions can be obtained by a covalent bond and noncovalent chemistries. Reprinted from [97] with permission from Springer Nature.

8. Role of Amines in the Stability of Adsorbents

Various types of amines have been widely employed to generate activated sites and improve the surface properties of INADs for environmental applications such as water treatment. Moreover, several authors have proposed that a high stability of the adsorbent is of great importance as it increases the efficiency of toxicant removal and reusability. In this aim, researchers estimated that addition of organic moieties bearing chelating groups on the support was effective to avoid the non-stabilization and aggregation of adsorbent particles [98]. Among these organic moieties, amines have attracted many researchers for the elaboration and functionalization of INADs through the chemical grafting of amines and/or its derivatives. In this regard, many works have shown that amine surface functionalization increases INAD stability and the number of reusability cycles. Figures 5 and 6 show an example of the mechanisms taking place during the process of APTES-functionalized graphene oxide (GO) [24]. APTES plays a crucial role in INAD stabilization based on graphene oxide as an adsorbent and it increases the immobilization yield of metallic nanoparticles. The results obtained with APTES-modified GO showed not only increases in the adsorption uptake toward organic pollutants but also improved reusability of the catalyst.

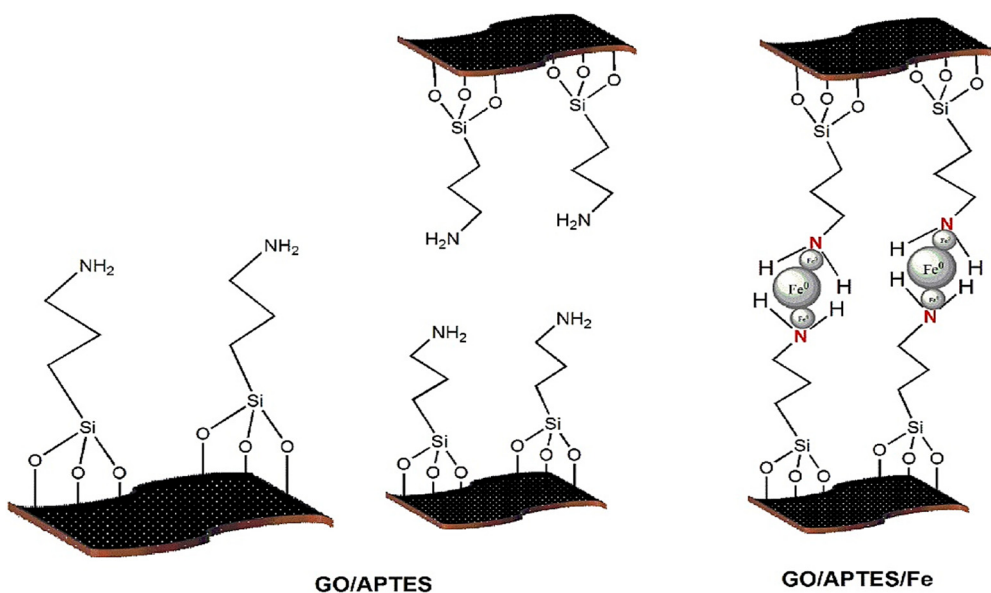


Figure 5. APTES for the stabilization and immobilization of iron nanoparticles onto GO adsorbent. Reprinted from [24] with permission from Elsevier.

The same trend was obtained for palladium stabilization on amine-functionalized zeolite. In other words, INAD materials can be stabilized by using amine as the organic surface in the organic-inorganic composite. Infrared spectroscopy measurements showed a marked change upon the incorporation of amines. This was observed by the slight decay in band intensity noticed for the 3400 cm^{-1} and 2919 cm^{-1} peaks associated to the asymmetric stretching vibrations of NH_2 and the C-H aliphatic groups. The authors explained these results by the significant role of amine insertion in the molecular structure of the INAD, which induced a compaction of the organic entanglement due to the occurrence of strong interactions between metal and amino groups M:NH₂ [99].

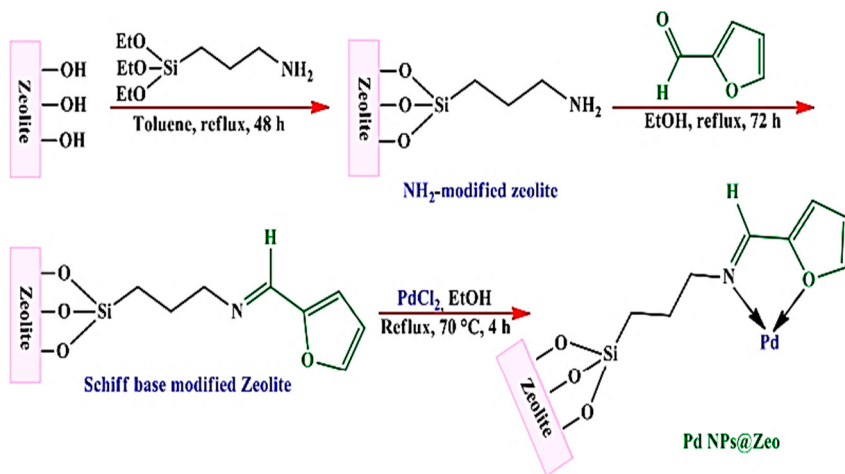


Figure 6. APTES for palladium immobilization at the zeolite surface. Reprinted from [100] with permission from Elsevier.

The above phenomenon is also reported in the literature for INAD based on metal nanoparticles, where the CH and OH groups involved interactions with NH₂ resulting in INAD stabilization [101]. These results clearly demonstrate that intercalation of amine-like APTES contributes to adsorbent stabilization due to strong interactions between the adsorbent and NH₂. Importantly, the thermal analysis demonstrated that untreated INAD has a low thermal stability, which is considered a drawback for many applications. How-

ever, amine addition played an interesting role by enhancing thermal stability. This was illustrated by the visible decrease in mass weight above 100 °C. Thus, chemical grafting of APTES increased the thermal stability of INAD, and induced more stable oxygen-functionalized groups, resulting in a higher temperature of around 500 °C to decompose the silanol groups or Si–O–Si bonds during amine surface functionalization of INAD. APTES and PAMAM as amine sources appear to be responsible for the thermal stability of the grafted materials. Concerning INAD durability, amines have a potential effect on INAD reusability. The results obtained on the removal of pollutants onto metal oxide, activated carbon, and fibrous materials revealed that immobilization of amine at the INAD surface had an interesting role as to INAD reusability and recyclability. Measurements of the catalytic activities of INAD showed that a copper oxide catalyst modified by the chemical grafting of amines could be recycled and reused several times for water treatment. This type of INAD was used more than seven times for 4-NP reduction, eight cycles for the removal of methylene blue (MB), five cycles for the elimination of malachite green (MG), and eight cycles for the removal of remazol red (RR) without visible decay in its catalytic capacity. This superior removal uptake is explained by the key role of APTES amine, which acts as an effective shield that prevents leaching and promotes material durability, and by the high stability of the catalysts (Figure 7). This was confirmed by the structure and thermal stability after the catalytic process. Both FT-IR and TGA analyses revealed no visible change compared with the unmodified counterpart (Figure 8).

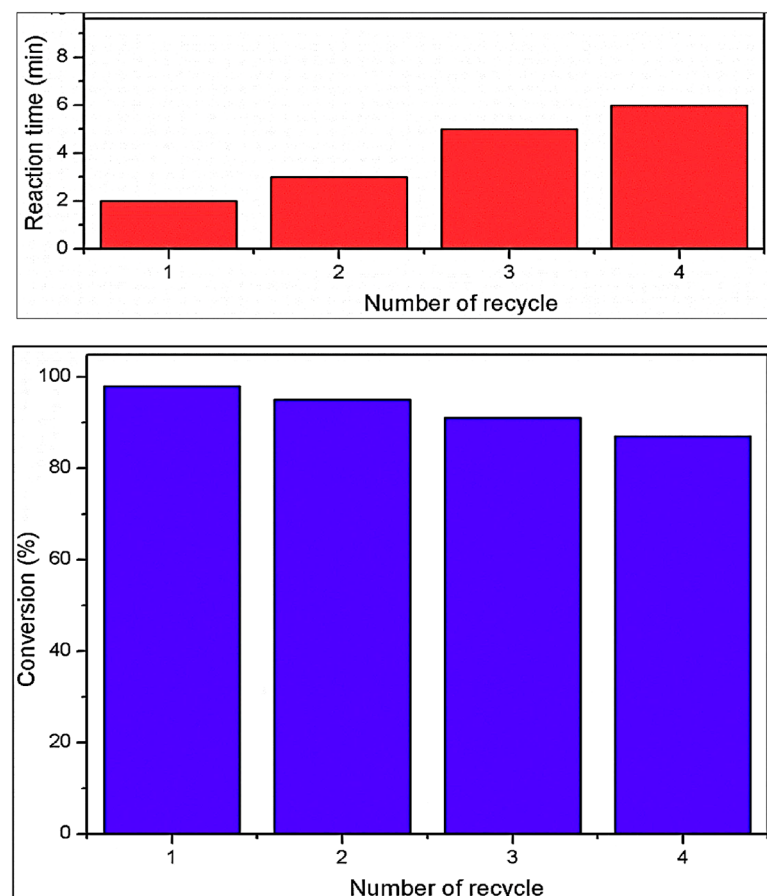


Figure 7. Reusability of amine-modified GO/APTES/Fe used as a catalyst for the reduction in 4-NP. Reprinted from [24] with permission from Elsevier.

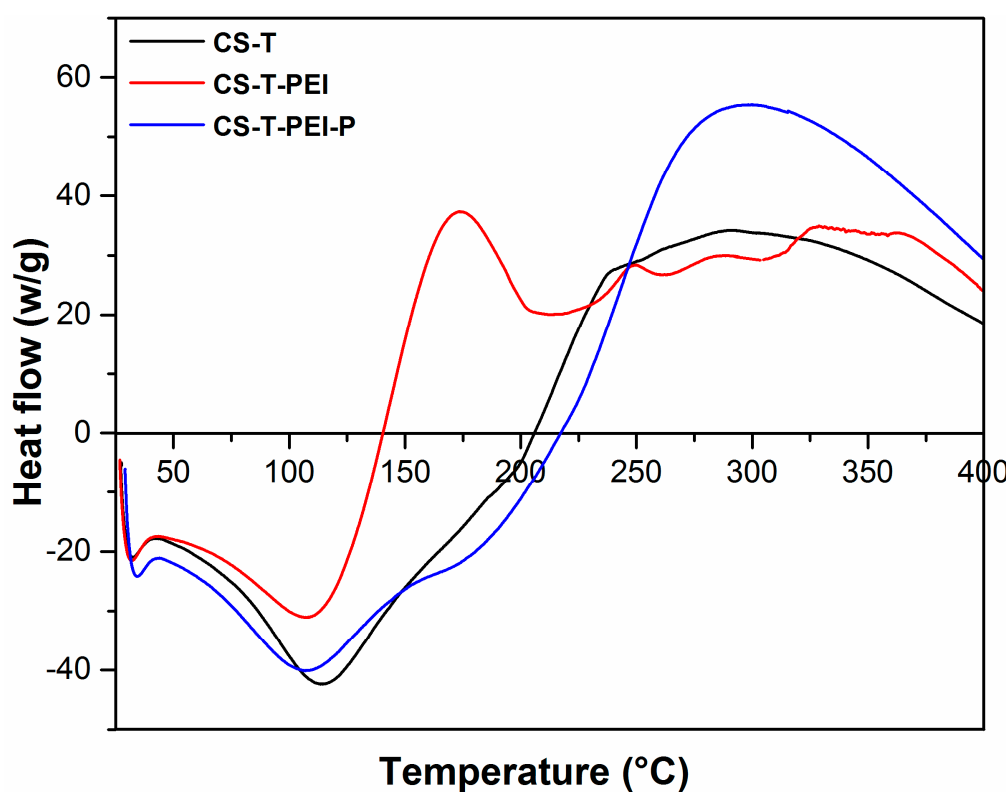


Figure 8. Amine grafting for thermal stability of biomass based on cocoa shell (CS). Reprinted from [4] with permission of the Royal Society of Chemistry.

9. Pollutant Removal by Amine-Grafted Inorganic Adsorbents

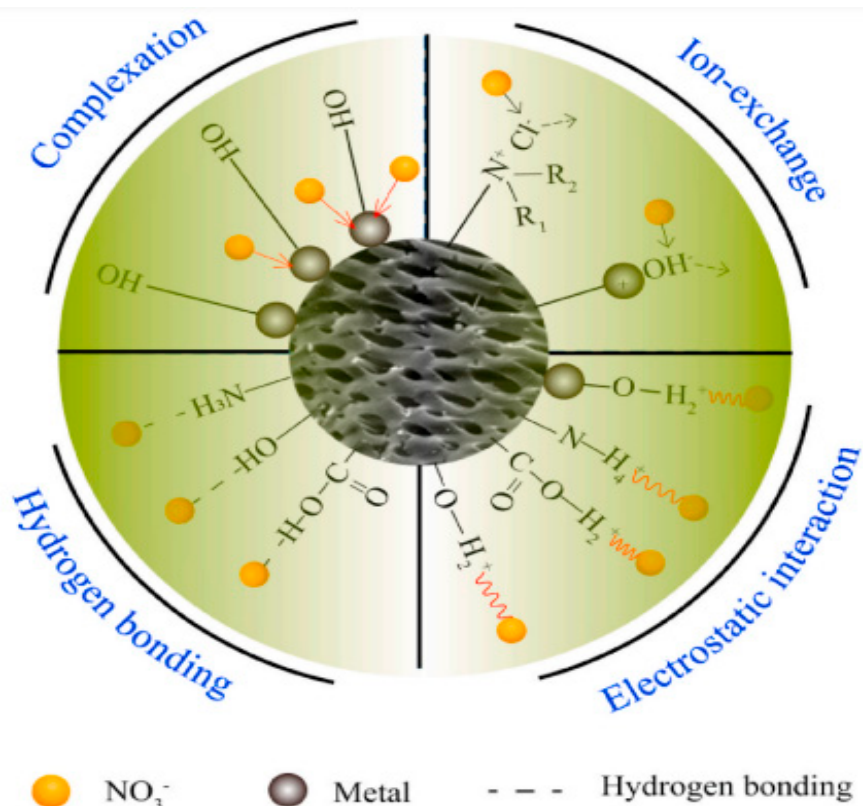
Tremendous amounts of minerals and organic pollutants can be found in water. This is why amine-modified INADs have attracted many scientists because they are effective for treating polluted waters and wastewater. This section studies the removal of various pollutants and bacteria using amine-grafted INADs.

9.1. Removal of Heavy Metals and Nitrates

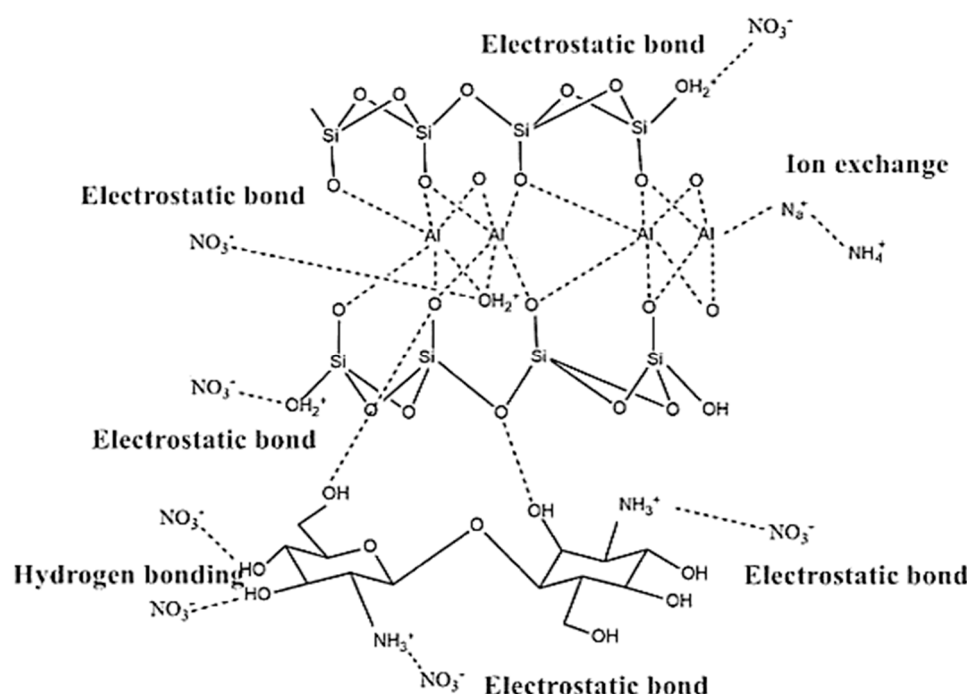
Table 3 summarizes the adsorption capacity of various INADs functionalized by amine grafting for removing dyes, nitrates, heavy metals, organic molecules, and pharmaceuticals from polluted water. The discussion starts with the removal of heavy metals and nitrate, which is a monovalent anion. Consequently, it allows positively charged surfaces or surfaces containing exchangeable anions to be effective adsorption sites. Liu et al. demonstrated that nitrate adsorption involved different kinds of adsorption processes such as electrostatic interactions, cation exchange, complexation, and hydrogen bonding [102]. These interactions depend on the composition, structure, and surface properties of the INAD and the adsorption conditions (Scheme 7).

The chemical functionalization of an INAD using aluminum-loaded activated carbon with grafting of the APTES for fluoride removal was studied by Bakhta et al. [103] and the sorption capacity of fluoride onto the functionalized INAD reached 92.0 mg g^{-1} . Fotsing et al. [104] prepared cocoa shell biomass via chemical grafting of APTES and PEI. This functionalized INAD was more effective for removing Cr(VI) and nitrates, with an approximate adsorption uptake of 100 mg g^{-1} . Furthermore, INADs showed affinity toward both nitrates and heavy metals as an interesting property of these adsorbents. This was explained by the role of amine immobilization at the INAD surface. In addition, the sorption of nitrate and Cr(VI) onto amine-modified biomass as a function of the pH improved from pH 2 to 5, with a maximum experimental adsorption capacity of 16.71 mg g^{-1} at pH 5. These results explained the competition between the amine and nitrate groups due to the interference of

silane present at the INAD surface. However, at higher pH values, competition between OH^- and NO_3^- may have occurred, resulting in decreased NO_3^- adsorption, and causing electrostatic repulsion between the surface and NO_3^- ions. Furthermore, Bao et al. [56] studied the removal of Zn(II) by functionalized $\text{Fe}_3\text{O}_4@\text{SiO}_2$ with amine groups. INADs were found to exhibit a sorption capacity around 169.5 mg g^{-1} at pH 5. Dindar et al. [105] modified INAD based on mesoporous silicate with a solution of APTES, and the final products were used to eliminate the Cr(VI), As(V), and Hg(II) ions. This investigation showed that the sorption efficiency depends on the number of amine groups present on each INAD surface. The APTES-modified INAD exhibited a sorption uptake around 47 mg g^{-1} , while the INAD treated with N-[3-trimethoxysilyl-propyl] ethylenediamine had a maximum sorption capacity around 140 mg g^{-1} at pH 1.7. The presence of amine groups at the INAD surface greatly improved the adsorption uptake of hazardous heavy metals and nitrates. In addition, they found out that the loading of more amine groups enhanced the adsorption capacity, as in the materials prepared with ethylenediaminepropyle salicylaldimine. In another study, modification of natural bentonite by anchoring APTES and 3,2-aminoethylaminopropyltrimetoxysilane (AEAPS) was prepared and applied to remove Pb(II) in aqueous solution [106]. Marjanović et al. [107] functionalized natural and acid-activated sepiolites by grafting, using the [3-(2-aminoethylamino)propyl] trimetoxysilane precursor. The material was used to remove chromium (VI) from aqueous solution. Different adsorption mechanisms can occur during heavy metal removal. The main adsorption phenomenon for heavy metals involves electrostatic attraction and hydrogen bonds. Keshvaroostchokami et al. [108] proved that a chitosan-based amine source improved the removal of pollutants such as nitrate and ammonia. Ammonia removal involved ion exchange, whereas nitrate removal implied hydrogen bonding and electrostatic bonding (Scheme 8).



Scheme 7. The possible adsorption of heavy metal onto INAD: illustration of the activated sites and their corresponding adsorption mechanism. Reprinted from [102] with permission from Elsevier.



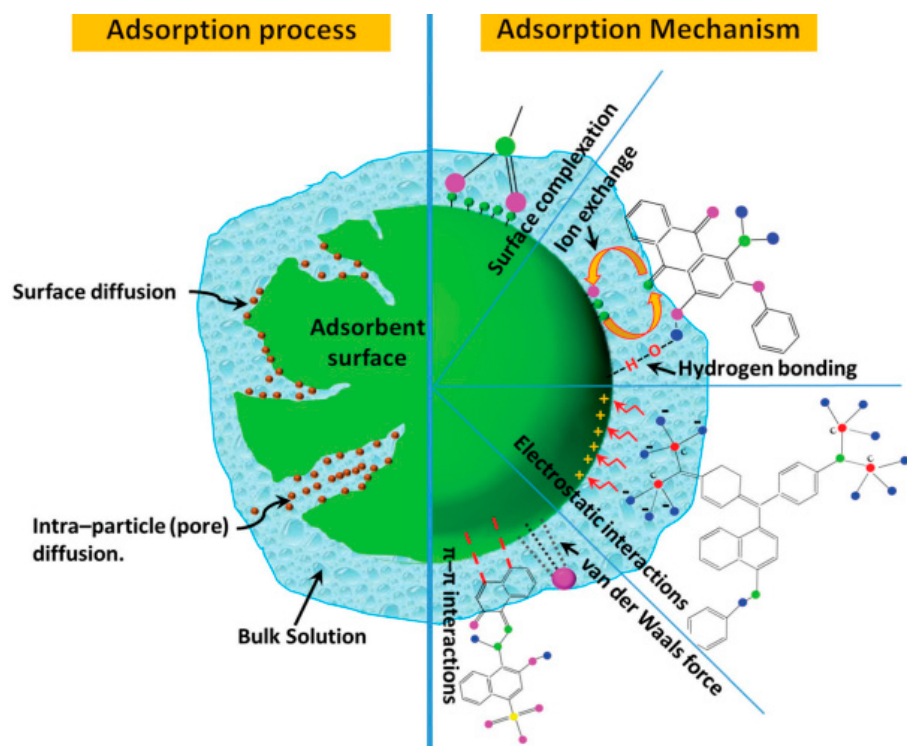
Scheme 8. Adsorption mechanism for the removal of ammonia and nitrate ions by chitosan-modified zeolite. Reprinted from [109] with permission from SAGE journals.

9.2. Removal of Dyes

Regarding the high amounts of untreated dyes (methylene blue, malachite green, crystal violet, remazol red, and others) discharged by various industries into the environment, amines have been considered a potential candidate for activating INADs for effective removal of these dyes. The control of dye degradation has traditionally been studied at different initial pollutant concentrations to measure the capacity of INADs to remove these toxic pollutants. A decreased absorbance of the solution over time reflected the progressive removal of the dyes from the solutions. By comparing the time required for reaching total dye removal by CuO-based unfunctionalized and amine-functionalized INADs, no dye was removed by the “raw” INAD. Nevertheless, amine-INAD showed a total dye removal in less than 2 min contact time [20,22]. Consequently, amine-loaded INAD displayed a superior adsorption uptake in comparison with its unmodified counterpart. This result is of great importance because it provides clear evidence that amine grafting onto INAD plays a key role in catalytic activities. In addition, the results revealed the important role played by amines in the stabilization of the INAD catalysts, as explained in the above sections. Xue et al. [65] grafted amine at the attapulgite surface to be used as an INAD for removing reactive dyes in aqueous solution. Amine grafting onto the INAD presented a very high adsorption capacity reaching 99.32% for various dyes such as MB and RR. The difference in the dye adsorption capacities was explained by the electrostatic attraction between reactive dyes and the protonated grafted amino groups. Lou et al. [110] reported the synthesis of APTES-Fe₃O₄/bentonite material and its application for MB adsorption. The maximum adsorption uptake was around 92 mg g⁻¹ as compared with its unmodified counterpart. Araghi et al. [111] reported the preparation of amino-loaded silica magnetite nanoparticles as an INAD, which illustrates the role of amine grafting in dye removal. Similarly, Morshed et al. investigated another type of INAD based on metal-fibrous materials and its modification with the PAMAM for cationic MB and MG dye elimination [112]. The adsorption capacities of the amine-grafted INAD were 49.48 mg g⁻¹ and 47.03 mg g⁻¹ for MB and MG, respectively. Furthermore, despite the role played by amine groups in dye removal, the porosity of the adsorbent should not be neglected during the sorption process. For cationic dyes, Laaz et al. [113] reported adsorption of red congo and anionic brilliant green

onto SBA-15 and amine-functionalized SBA-15 as INADs. Red congo removal significantly depended on the number of grafted amine functional groups rather than on the porosity of the material. Therefore, increasing the number of amine groups at the INAD surface can improve the capacities for dye adsorption. Additionally, the hydrophilic character and the bond interactions between dyes and amine functional groups explain the high adsorption capacities of amino-silicate-based INADs.

The adsorption of dyes from contaminated water onto the surface of an adsorbent can be achieved via various adsorption mechanisms [114]. Dye adsorption onto INADs involves many processes such as surface complexation, electrostatic interactions, van der Waals forces, surface diffusion, and intraparticle pore diffusion, as shown in Scheme 9.



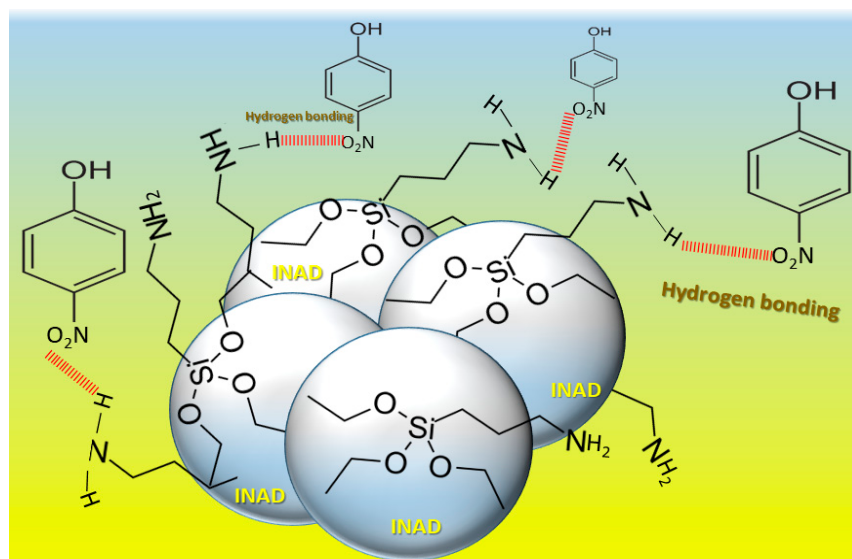
Scheme 9. Adsorption processes and mechanisms for dye removal from bulk liquid. Reprinted from [114] with permission from Elsevier.

9.3. Elimination of Organic Pollutants

The treatment of hazardous organic compounds present in wastewaters has attracted great attention, and the control of water pollution has become one of the major challenges worldwide. Major classes of nitrophenolic molecules act as organic pollutants when they are released in water by numerous industries [115–118]. Amine-grafted INADs have shown positive results for eliminating these organic pollutants. Furthermore, methods for reducing and removing these pollutants, e.g., adsorption and catalytic reduction, have been considered the most effective techniques for water depollution. Bouazizi et al. studied the removal of 4-NP organic dye via catalytic reduction in graphene oxide (GO) and APTES-functionalized GO as INAD materials [24]. Measurements of the UV-absorption bands showed a strong decay of the 400 nm band for 4-NP and increase in the 290 nm peak for 4-AP. Importantly, this effect was even more pronounced in the presence of APTES amine. This provides evidence of the beneficial contribution of amine grafting for both catalytic reduction and nanoparticle immobilization. Catalytic performance was related to the key role of APTES grafting in enhancing the electron transfer from the INAD surface to the nitro group of 4-NP [119–121]. It is worth noting that the reduction yield of the organic molecules was around 97.5% in less than 2 min, suggesting that amine-functionalized catalysts can rapidly generate 4-AP as ecofriendly molecules [122,123]. As previously stated, the grafting

of APTES improved the removal of toxic pollutants. The slight decrease in the concentration of 4-NP may be associated with the adsorption behavior of the 4-NP molecules onto the amino-INAD [124]. Interestingly, kinetic studies on APTES-modified INADs showed a constant rate k around 0.481 min^{-1} , superior to those of unmodified INAD. These results can be explained by the existence of a strong amino/support interaction effect between the amine groups (APTES) and the INAD (GO sheets) [125].

The improvement of the catalytic properties was further associated to organic pollutant diffusion towards the solid surface of the INAD. Similarly, works on metal-fibrous material-based INADs and their amine-functionalized counterpart for organic element removal showed that APTES grafting was key to improving electron transfer in link with the catalytic capacity. To verify the role played by amines in the depollution of water from organic molecules, control experiments were performed to study the reduction in 4-NP by calculating the rate constant. The time course of catalysis strongly depended on the post-treatment steps, and evidenced a positive effect of amine grafting onto INAD, as supported by a higher value of k . Finally, the removal of organic molecules by INADs can occur via hydrogen bonding. More particularly, adsorption of organic contaminants with terminal NO_2 , SO_2 , and CO_2 onto amine-modified INAD involves hydrogen bonding (Scheme 10).



Scheme 10. Mechanism of adsorption onto amine-grafted silicate-based material.

9.4. Degradation of Mixtures of Pollutants

Mixtures of organic molecules and dyes can be released in the environment in the form of industrial effluents, and this complicates their removal during the water remediation process. In this regard, elimination of these hazardous molecules is of great importance, as it is an urgent issue. Following the same water treatment protocol as mentioned in the above sections, various amine-modified INADs have been used for removing pollutant mixtures. INADs had an affinity toward the adsorption of mixtures of organic pollutants and dyes (Figure 9). An aqueous solution containing a mixture of nitrophenol and dyes was typically employed to evaluate the adsorption capacity of INADs functionalized by APTES grafting (Table 3). The pollutants fully disappeared within a few minutes, suggesting that INADs are efficient for removing pollutant mixtures. A comparison of the removal of different organic molecules such as nitrophenol and MB dyes demonstrated that nitrophenol required more time for its complete elimination. However, these results showed that amine-functionalized INADs are more efficient for removing organic pollutants than for removing dyes. This was explained by the unavoidable protonation of 4-NP groups which could favor the adsorption of dye.

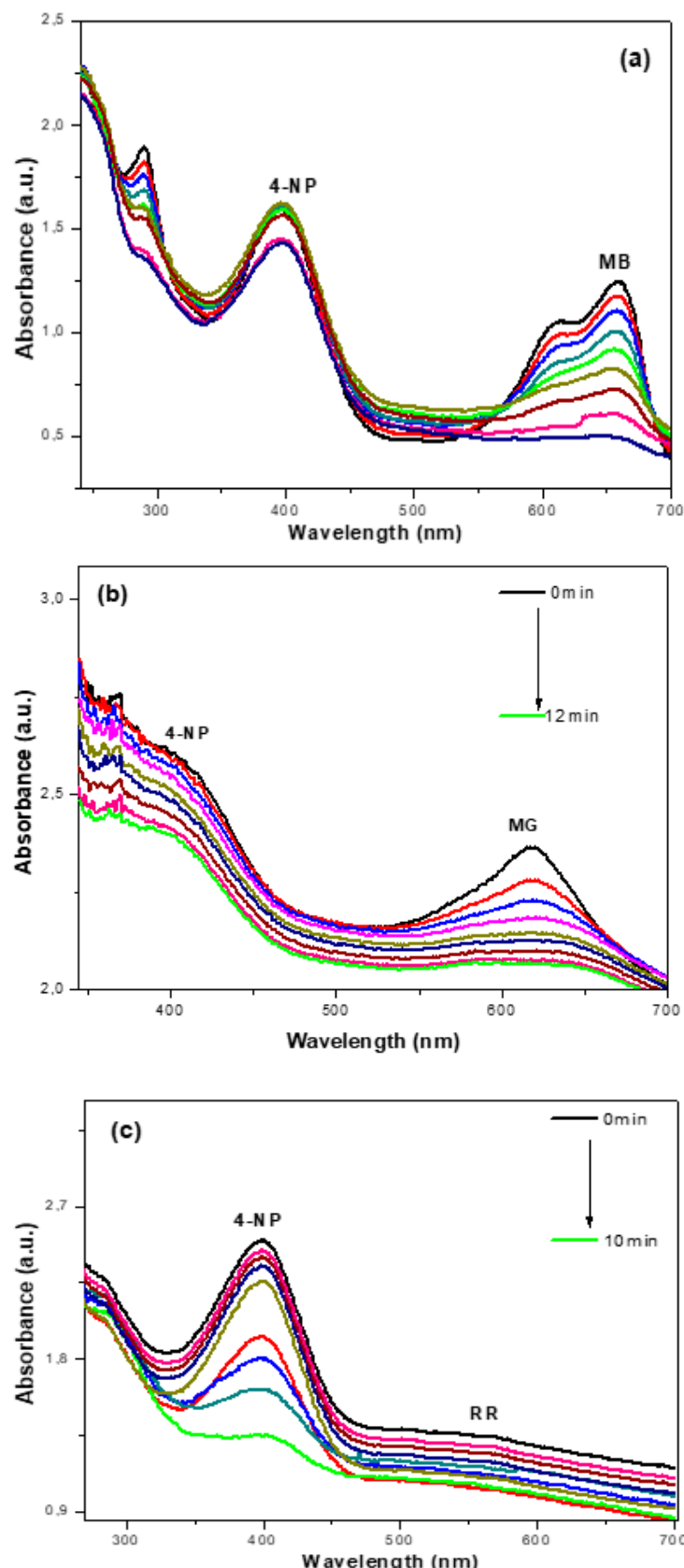


Figure 9. Metal–organic fibrous materials for the removal of methylene blue (MB), red remazol (RR), malachite green (MG), and 4-nitrophenol (4-NP) as mixtures of pollutants: 4-NP + MB (a); 4-NP + MG (b) and 4-NP + RR (c). Reprinted from [19] with permission from Elsevier.

Table 3. Pollutant adsorption capacity of amine functionalized-INAD materials.

Inorganic Adsorbents (INADs)	Grafted Amines	Removed Pollutants	Adsorption Capacity (mg g^{-1})	Reference
Graphene oxide	PAMAM	Nitrate	1025.9	[126]
Porous rice husk silica	PEI	Nitrate	94.5	[9]
Nanochitosan/ clinoptilolite	PEHA	Nitrate	277.8	[127]
Magnetized mesoporous silica (SBA-15)	APTES	Nitrate	44.9	[128]
Polystyrene microspheres	hexamethylenetetramine	Nitrate	221.8	[129]
Cocoa shell	APTES	Nitrate Cr(IV)	16.9 24.8	[104]
Magnetic nanoparticules Fe_3O_4 SiO_2	APTES	Zn (II)	270.3	[130]
Mesoporous silica SBA-15	APTES aminopropyl and <i>N</i> - propylsalicylaldimine	Cr (V) As (V) Hg (II)	64.2 16.3 7.0	[105]
Bentonite	APTES and 3,2-aminoAEAPS	Pb (II) Pb (II)	27.6 29.5	[106]
Acid-activated sepiolites	AEAPS	Cr (VI)	60	[107]
Kaolin composite	Acrylamide	Cs (II) Co(II)	19.9 10.5	[40]
Clay (heulandite)	Chitosan	Cu(II) As(V)	17.2 5.9	[44]
Chitosan/PVA/PES	$\text{Fe}_3\text{O}_4-\text{NH}_2$	Cr(VI) Pb(II)	509.7 525.8	[45]
Magnetic graphene composite	EDA	Cr(VI) Pb(II) Hg(II) Cd(II) Ni(II)	17.3 27.9 23.0 27.9 22.0	[46]
Fe_3O_4	HMD	Cr (VI)\Ni (II)	232.5 222.1	[47]
Magnesium ferrite nanoparticles (MgFe_2O_4)	Mesoporous amine NH_2	Pb (II)	135.1	[48]
$\text{Fe}_3\text{O}_4/\text{NaP}$ zeolite nanocomposite	APTES	Pb(II) Cd(II)	181.8 50.2	[49]
Magnetic illite-smectite clay	APTES	Pb(II)	227.8	[50]
Core-shell magnetic nanoparticle	APTES and NTA	Cu (II) Sb (III)	55.6 51.1	[52]
Chitosan-coated magnetite	Hydrazinyl amine	Ni(II) Pb(II)	3.9 2.6	[53]
Maghemite nanoparticles	Glycine	Cu (II)	625	[54]
Magnetic bentonite/Co $\text{Fe}_2\text{O}_4@\text{MnO}_2$	APTES	Cd(II)	115.8	[57]
Clay (palygorskite)	APTES	Reactive red 3BS	34.2	[79]
Bentonite	APTES- Fe_3O_4	Methylene blue	91.8	[110]
Modified fibrous nonwoven	PAMAM	Methylene blue, malachite green	49.5 47.0	[18]

Table 3. Cont.

Inorganic Adsorbents (INADs)	Grafted Amines	Removed Pollutants	Adsorption Capacity (mg g ⁻¹)	Reference
Mesoporous material SBA-15	APTES	Red congo, brilliant green	25.5 56.3	[113]
Activated carbon	DETA	Phenol	18.1	[58]
Magnetic bamboo-based activated carbon	EDA	Ciprofloxacin, norfloxacin	245.6 293.2	[59]
Polyester fabrics (PET)	APTES PAMAM	4-nitrophenol (4-NP)	293.3 269.9	[60]
Montmorillonite clay	Poly(4-vinylpyridine)	Selenate, Eosin Y dye methyl blue	176.1 8.5 156.9	[41]
Montmorillonite	Quarternized poly vinylpyridinium-co-styrene	Diclofenac	100.6	[43]

10. Amines for Biomedical Applications

Day after day in the past decades, the use of antibiotics has increased and the number of resistant bacterial strains has increased too. On the path of searching for effective materials with antibacterial properties, amine-modified INADs displayed an interesting behavior toward inhibition of bacteria. The antimicrobial properties of amine-functionalized INADs were evaluated by diffusivity and inhibitory tests towards the two Gram+ and Gram– bacterial strains *Staphylococcus epidermidis* and *Escherichia coli*, respectively. Bouazizi et al. studied the antibacterial capacity of copper oxide modified by amine intercalation on the growth of *E. coli* and *S. epidermidis*. Optical density measurements showed that antibacterial activity occurred when a state of partial CuO dissolution and Cu⁺ cation release was reached. Interestingly, the addition of amine-based DEA at the CuO surface highly increased the antibacterial capacity, suggesting that amine groups may restrict the release of Cu⁺ cation [17,19,21]. Subsequently, chemical grafting of -NH- can penetrate the cell and release the cation inside, and then damage the bacterium. In other words, the protonation of amine groups is attributed to the antibacterial property, involving sufficiently strong electrostatic interactions with the negatively charged bacterial membranes, and resulting in inhibited bacterial growth [17,21]. Therefore, antibacterial activity was improved, evidencing the key role of amine functionalization for CuO nanosheets. In the same vein, results obtained with CuO-Si-S-NH₂ showed that greater bacterial inhibition was observed after APTES grafting. Researchers explained that the number of free electrons at the nanosheet interface increased following amine addition, and made the resulting INAD more efficient in killing bacteria such as *S. epidermidis* and *E. coli*. These results were confirmed using amine-functionalized metal-fibrous materials, indicating that -NH₂ grafting was involved in damaging the bacterial cells: optical density measurements went down to zero (Figure 10). Consequently, the chemical grafting of amines is the main parameter that endows metal oxides with antibacterial activity against both Gram+ and Gram– bacteria. The mechanism can be explained as follows: the surface area of the nanoparticles adheres to powder strands which in turn increases the contact between the powder and the bacteria. Meanwhile, the amine groups increase the junction with the powder particles, and thus the contact with the bacteria is prolonged. A longer contact time between nanoparticles and bacteria causes more damage to the bacteria so that the antibacterial capacity is improved. The antibacterial activity is also explained by the oxygen species generated by the reaction, such as H₂O₂ and O₂•. More of them are produced after the intercalation of amine molecules. Therefore, this improvement is closely related to the Cu, Si, and N elements.

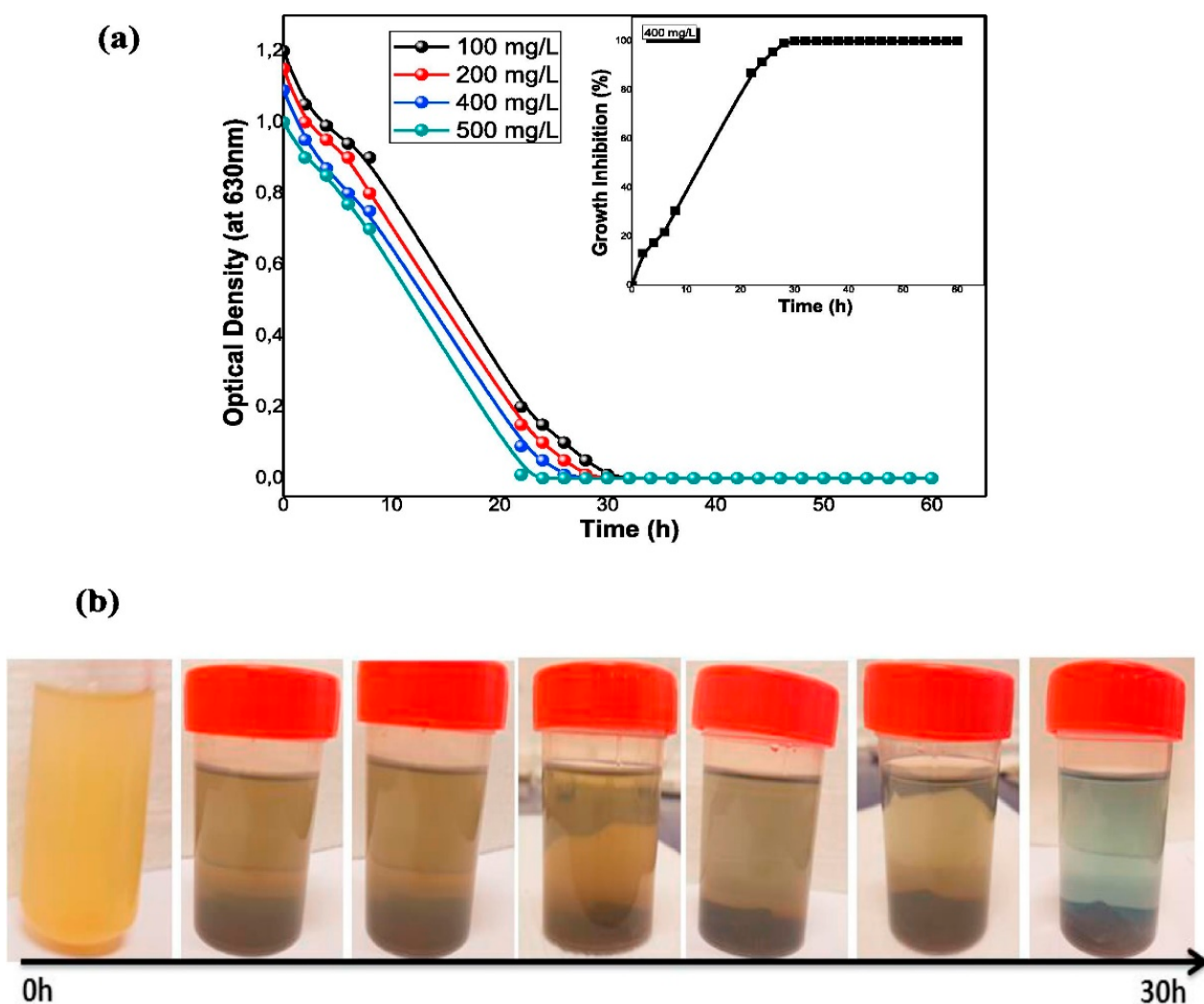


Figure 10. Optical density (a) and changes in the turbidity of the solution (b) in a cell growth inhibition experiment using INAD against a mixture of *E. coli* and *S. epidermidis*. Reprinted from [18] with permission from Elsevier.

Amine surface functionalization of INADs caused the rupture of bacterial cells, their shrinkage, and their death. This confirms the antibacterial effect of the amine-functionalized samples. Another work reached the same conclusion using trimethylamine (TEA)-grafted zeolite. Figure 11 summarizes the inhibition zone diameter values of untreated and INAD-treated solution. The unmodified INAD possessed antibacterial activity against both bacteria. However, when amine groups were inserted within the INAD structure, the antibacterial activity was further enhanced. Measurements of the diameter of the inhibition zone showed 27.9% and 64.9% increases for *E. coli* and *S. aureus*, respectively. This improvement in the antibacterial capacity was attributed to the synergistic effects of the positively charged protonated amine groups grafted onto the INAD. This behavior is in good agreement with the literature [131–133]. According to these studies, such increases in the positively charged surfaces can actually increase the interaction between the INAD and the negatively charged bacterial cells.

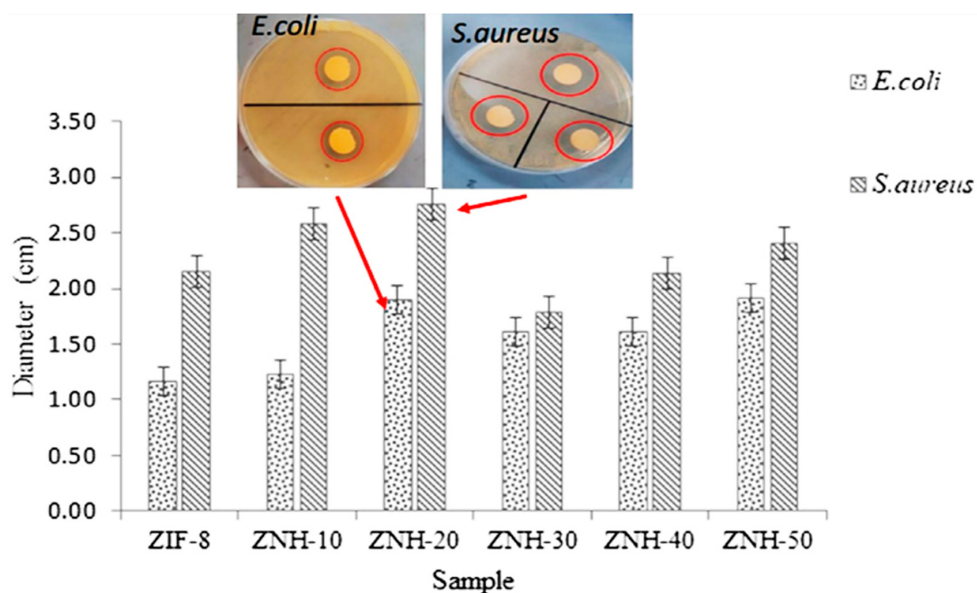


Figure 11. Zone of inhibition (cm) of each sample against *E. coli* and *S. aureus*. Insets are the respective zones of inhibition of the ZNH-20 sample. Reprinted from [78] with permission from Elsevier.

Based on the morphology of bacterial cells, researchers clearly observed and controlled these antibacterial properties. In its normal state, *E. coli* appears as a rod with an intact cell-shaped structure [134]. After amine grafting onto the INAD surface, holes were observed on the bacterial membranes. Therefore, amine addition disrupted the bacterial membrane, causing leakage of the bacterial cytoplasmic materials [135]. This behavior is well documented for *E. coli* as compared with *S. aureus*. In similar conditions, the morphology of *S. aureus* did not appear to be damaged (Figure 12). This might be due to a different killing mechanism in which the damage mostly affected the proteins, lipids, or inner components of the bacteria, rather than the bacterial membrane [136]. The different mechanisms could be due to the different membranes of *E. coli* and *S. aureus*. The thicker membrane of Gram+ bacteria better protects the membrane from damage [135,136].

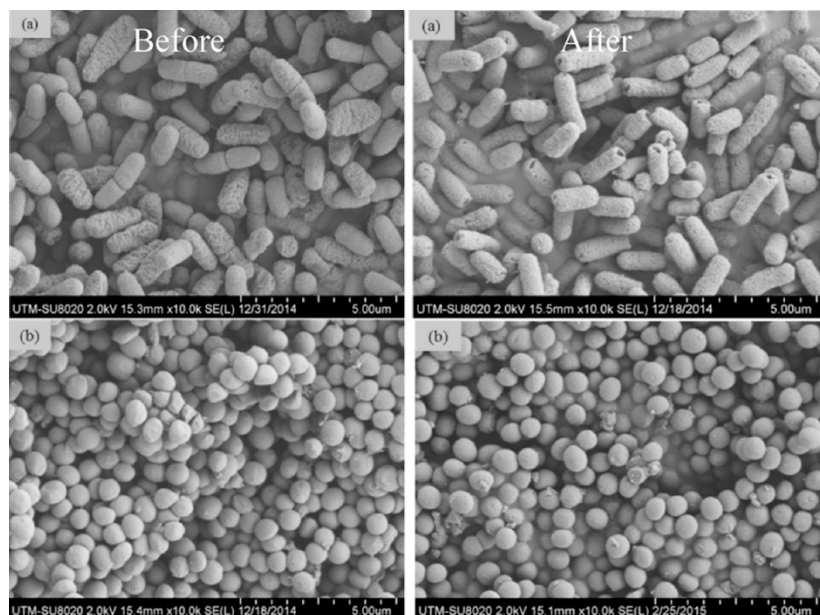


Figure 12. Morphology of (a) *E. coli* and (b) *S. aureus* before and after the antibacterial assay. Reprinted from [133] with permission from Elsevier.

11. Conclusions

Various inorganic adsorbents (INADs) based on metal oxide, metal-loaded fibrous materials, graphene oxide, metal–organic frameworks, silica, and metal-loaded biomass were functionalized by amine grafting for improved removal of pollutants in wastewater and antibacterial activity. Chemical functionalization of INADs via the grafting of amine depends on many parameters such as the nature of the solvent, the temperature, the amount of water, and the quantity of amine precursors. Amines are an effective agent for INADs because they induce superior activated sites at the surface of materials, which are very suitable for various applications. Due to the key roles of amines, INADs have been successfully used for adsorbing and removing heavy metals, dyes, organic molecules, mixtures of pollutants, and bacteria from water. Amine fixation can occur via covalent interactions, hydrogen bonding, and electrostatic interactions. Further kinds of amine grafting will be very useful and can play a key role to enhance both catalytic and antibacterial activities. Amine-functionalized INADs can be employed to produce highly activated sites at the grafted surface, which can act as supplementary activated sites. Furthermore, amine-modified INADs enhance antibacterial activity due to the presence of highly reactive oxygen species. The next challenge will be to upscale the experiments towards an industrial scale. Finally, the use of amine-grafted INADs for water disinfection is expected to be explored in the future.

Author Contributions: Conceptualization, N.B., B.S., and J.V.; methodology, N.B.; software, N.B., B.S., and J.V.; validation, B.S., and J.V.; formal analysis, N.B., B.S., and J.V.; investigation, N.B., B.S., and J.V.; resources, J.V., and F.L.D.; data curation, N.B., B.S., and J.V.; writing—original draft preparation, N.B.; writing—review and editing, N.B., B.S., and J.V.; visualization, N.B., B.S., and J.V.; supervision, J.V.; project administration, J.V., and F.L.D.; funding acquisition, J.V., and F.L.D. All authors have read and agreed to the published version of the manuscript.

Funding: This work was partially supported by INSA Rouen, Rouen University, CNRS, Labex SynOrg (ANR-11-LABX-0029), the European Regional Development Fund (ERDF) N° HN0001343, the graduate school for research Xl-Chem (ANR-18-EURE-0020 XL CHEM), the Normandy region (CBS network) and the Grand Evreux Agglomeration.

Conflicts of Interest: The authors declare no conflict of interest.

Nomenclature

AEAPS	3,2-aminoethylaminopropyltrimethoxysilane
APTES	3-aminopropyltriethoxysilane
BDTA	benzyldimethyltetradecylammonium
CPTES	3-chloropropyltriethoxysilane
DEA	Diethanolamine
DETA	Diethylenetriamine
EDA	Ethylenediamine
PEI	Polyethyleneimine
HMD	Hexamethylenediamine
DAN	1,5-diaminonaphthalene
APTMS	3-aminopropyltrimethoxysilane
DETA	Diethylenetriamine
PAMAM	Polyamidoamine-NH ₂
MOFs	Metal–organic frameworks
ATP	2-aminoterephthalic acid
3APPA	3-aminopropylphosphonic acid
INAD	Inorganic adsorbent
MOx	Metal oxide
TEPA	Tetraethylpentamine
NTA	Nitrilotriacetic acid

TETA	Triethylenetetraamine
PATP	p-aminothiophenol
PEHA	Pentaethylenhexamine
TEA	Trimethylamine
GO	Graphene oxide
AC	Activated carbon
3APPA	3-aminopropylphosphonic acid
3PPA	3-propylphosphonic acid

References

- Vörösmarty, C.J.; McIntyre, P.B.; Gessner, M.O.; Dudgeon, D.; Prusevich, A.; Green, P.; Glidden, S.; Bunn, S.E.; Sullivan, C.A.; Liermann, C.R.; et al. Global threats to human water security and river biodiversity. *Nature* **2010**, *467*, 555–561. [CrossRef] [PubMed]
- Ayad, M.M.; El-Nasr, A.A. Adsorption of cationic dye (methylene blue) from water using polyaniline nanotubes base. *J. Phys. Chem. C* **2010**, *114*, 14377–14383. [CrossRef]
- Lin, J.; Zhang, X.; Li, Z.; Lei, L. Biodegradation of Reactive blue 13 in a two-stage anaerobic/aerobic fluidized beds system with a *Pseudomonas* sp. isolate. *Bioresour. Technol.* **2010**, *101*, 34–40. [CrossRef]
- Chakrabarti, S.; Dutta, B.K. Photocatalytic degradation of model textile dyes in wastewater using ZnO as semiconductor catalyst. *J. Hazard. Mater.* **2004**, *112*, 269–278. [CrossRef] [PubMed]
- Rajeshwar, K.; Osugi, M.; Chanmanee, W.; Chenthamarakshan, C.; Zanoni, M.V.B.; Kajitvichyanukul, P.; Krishnan-Ayer, R. Heterogeneous photocatalytic treatment of organic dyes in air and aqueous media. *J. Photochem. Photobiol. C Photochem. Rev.* **2008**, *9*, 171–192. [CrossRef]
- Gözmen, B.; Kayan, B.; Gizar, A.M.; Hesenov, A. Oxidative degradations of reactive blue 4 dye by different advanced oxidation methods. *J. Hazard. Mater.* **2009**, *168*, 129–136. [CrossRef]
- Lazaratou, C.; Vayenas, D.; Papoulis, D. The role of clays, clay minerals and clay-based materials for nitrate removal from water systems: A review. *Appl. Clay Sci.* **2020**, *185*, 105377. [CrossRef]
- Lazaridis, N.; Asouhidou, D. Kinetics of sorptive removal of chromium(VI) from aqueous solutions by calcined Mg-Al-CO₃ hydrotalcite. *Water Res.* **2003**, *37*, 2875–2882. [CrossRef]
- Suzaimi, N.D.; Goh, P.S.; Malek, N.A.N.N.; Lim, J.W.; Ismail, A.F. Performance of branched polyethyleneimine grafted porous rice husk silica in treating nitrate-rich wastewater via adsorption. *J. Environ. Chem. Eng.* **2019**, *7*, 103235. [CrossRef]
- Srivastava, V.; Choubey, A.K. Investigation of adsorption of organic dyes present in wastewater using chitosan beads immobilized with biofabricated CuO nanoparticles. *J. Mol. Struct.* **2021**, *1242*, 130749. [CrossRef]
- Abdulhameed, A.S.; Mohammad, A.-T.; Jawad, A.H. Application of response surface methodology for enhanced synthesis of chitosan tripolyphosphate/TiO₂ nanocomposite and adsorption of reactive orange 16 dye. *J. Clean. Prod.* **2019**, *232*, 43–56. [CrossRef]
- Abdulhameed, A.S.; Jawad, A.H.; Mohammad, A.-T. Synthesis of chitosan-ethylene glycol diglycidyl ether/TiO₂ nanoparticles for adsorption of reactive orange 16 dye using a response surface methodology approach. *Bioresour. Technol.* **2019**, *293*, 122071. [CrossRef] [PubMed]
- Bhatkhande, D.S.; Pangarkar, V.G.; Beenackers, A.A.C.M. Photocatalytic degradation for environmental applications—A review. *J. Chem. Technol. Biotechnol.* **2002**, *77*, 102–116. [CrossRef]
- Tilt, B. The politics of industrial pollution in rural China. *J. Peasant. Stud.* **2013**, *40*, 1147–1164. [CrossRef]
- Antoniadou, M.; Panagiotopoulou, P.; Kondarides, D.I.; Lianos, P. Photocatalysis and photoelectrocatalysis using nanocrystalline titania alone or combined with Pt, RuO₂ or NiO co-catalysts. *J. Appl. Electrochem.* **2012**, *42*, 737–743. [CrossRef]
- Nazari, P.; Gharibzadeh, S.; Ansari, F.; Nejand, B.A.; Eskandari, M.; Kohnehpoushi, S.; Ahmadi, V.; Salavati-Niasari, M. Facile green deposition of nanostructured porous NiO thin film by spray coating. *Mater. Lett.* **2017**, *190*, 40–44. [CrossRef]
- Bouazizi, N.; Bargougui, R.; Thebault, P.; Clamens, T.; Desriac, F.; Fioretti, F.; Ladam, G.; Morin-Grognet, S.; Mofaddel, N.; Lesouhaitier, O.; et al. Development of a novel functional core-shell-shell nanoparticles: From design to anti-bacterial applications. *J. Colloid Interface Sci.* **2018**, *513*, 726–735. [CrossRef]
- Nabil, B.; Morshed, M.N.; Ahmida, E.A.; Nemeshwaree, B.; Christine, C.; Julien, V.; Olivier, T.; Abdelkrim, A. Development of new multifunctional filter based nonwovens for organics pollutants reduction and detoxification: High catalytic and antibacterial activities. *Chem. Eng. J.* **2019**, *356*, 702–716. [CrossRef]
- Nabil, B.; Ahmida, E.A.; Christine, C.; Julien, V.; Abdelkrim, A. Polyfunctional cotton fabrics with catalytic activity and antibacterial capacity. *Chem. Eng. J.* **2018**, *351*, 328–339. [CrossRef]
- Bouazizi, N.; Vieillard, J.; Thebault, P.; Desriac, F.; Clamens, T.; Bargougui, R.; Couvrat, N.; Thoumire, O.; Brun, N.; Ladam, G.; et al. Silver nanoparticle embedded copper oxide as an efficient core-shell for the catalytic reduction of 4-nitrophenol and antibacterial activity improvement. *Dalton Trans.* **2018**, *47*, 9143–9155. [CrossRef] [PubMed]
- Vieillard, J.; Bouazizi, N.; Morshed, M.N.; Clamens, T.; Desriac, F.; Bargougui, R.; Thebault, P.; Lesouhaitier, O.; Le Derf, F.; Azzouz, A. CuO Nanosheets Modified with Amine and Thiol Grafting for High Catalytic and Antibacterial Activities. *Ind. Eng. Chem. Res.* **2019**, *58*, 10179–10189. [CrossRef]

22. Fotsing, P.N.; Bouazizi, N.; Woumfo, E.D.; Mofaddel, N.; Le Derf, F.; Vieillard, J. Investigation of chromate and nitrate removal by adsorption at the surface of an amine-modified cocoa shell adsorbent. *J. Environ. Chem. Eng.* **2020**, *9*, 104618. [[CrossRef](#)]
23. Bouazizi, N.; Vieillard, J.; Bargougui, R.; Couvrat, N.; Thoumire, O.; Morin, S.; Ladam, G.; Mofaddel, N.; Brun, N.; Azzouz, A.; et al. Entrapment and stabilization of iron nanoparticles within APTES modified graphene oxide sheets for catalytic activity improvement. *J. Alloys Compd.* **2019**, *771*, 1090–1102. [[CrossRef](#)]
24. Bouazizi, N.; Boudharaa, T.; Bargougui, R.; Vieillard, J.; Ammar, S.; Le Derf, F.; Azzouz, A. Synthesis and properties of ZnO-HMD@ZnO-Fe/Cu core-shell as advanced material for hydrogen storage. *J. Colloid Interface Sci.* **2017**, *491*, 89–97. [[CrossRef](#)] [[PubMed](#)]
25. Bouazizi, N.; Ajala, F.; Bettaibi, A.; Khelil, M.; Benghnia, A.; Bargougui, R.; Louhichi, S.; Labiad, L.; Ben Slama, R.; Chaouachi, B.; et al. Metal-organo-zinc oxide materials: Investigation on the structural, optical and electrical properties. *J. Alloys Compd.* **2016**, *656*, 146–153. [[CrossRef](#)]
26. Bouazizi, N.; Bargougui, R.; Boudharaa, T.; Khelil, M.; Benghnia, A.; Labiad, L.; Ben Slama, R.; Chaouachi, B.; Ammar, S.; Azzouz, A. Synthesis and characterization of SnO 2-HMD-Fe materials with improved electric properties and affinity towards hydrogen. *Ceram. Int.* **2016**, *42*, 9413–9418. [[CrossRef](#)]
27. Kumar, R.V.; Diamant, Y.; Gedanken, A. Sonochemical Synthesis and Characterization of Nanometer-Size Transition Metal Oxides from Metal Acetates. *Chem. Mater.* **2000**, *12*, 2301–2305. [[CrossRef](#)]
28. An, W.-J.; Thimsen, E.; Biswas, P. Aerosol-Chemical Vapor Deposition Method For Synthesis of Nanostructured Metal Oxide Thin Films With Controlled Morphology. *J. Phys. Chem. Lett.* **2010**, *1*, 249–253. [[CrossRef](#)]
29. Chequer, F.M.D.; de Oliveira, G.A.R.; Ferraz, E.R.A.; Cardoso, J.C.; Zanoni, M.V.B.; de Oliveira, D.P. Textile Dyes: Dyeing Process and Environmental Impact. *Eco-Friendly Text. Dye. Finish.* **2013**, *6*, 151–176.
30. Cai, Z.; Sun, Y.; Liu, W.; Pan, F.; Sun, P.; Fu, J. An overview of nanomaterials applied for removing dyes from wastewater. *Environ. Sci. Pollut. Res.* **2017**, *24*, 15882–15904. [[CrossRef](#)]
31. Mu, Y.; Rabaey, K.; Rozendal, R.A.; Yuan, Z.; Keller, J. Decolorization of Azo Dyes in Bioelectrochemical Systems. *Environ. Sci. Technol.* **2009**, *43*, 5137–5143. [[CrossRef](#)]
32. Chen, G. Electrochemical technologies in wastewater treatment. *Sep. Purif. Technol.* **2004**, *38*, 11–41. [[CrossRef](#)]
33. Vieillard, J.; Bouazizi, N.; Bargougui, R.; Fotsing, P.N.; Thoumire, O.; Ladam, G.; Brun, N.; Hochepied, J.-F.; Woumfo, E.D.; Mofaddel, N.; et al. Metal-inorganic-organic core-shell material as efficient matrices for CO₂ adsorption: Synthesis, properties and kinetic studies. *J. Taiwan Inst. Chem. Eng.* **2019**, *95*, 452–465. [[CrossRef](#)]
34. Bargougui, R.; Bouazizi, N.; Brun, N.; Fotsing, P.N.; Thoumire, O.; Ladam, G.; Woumfo, E.D.; Mofaddel, N.; Le Derf, F.; Vieillard, J. Improvement in CO₂ adsorption capacity of cocoa shell through functionalization with amino groups and immobilization of cobalt nanoparticles. *J. Environ. Chem. Eng.* **2018**, *6*, 325–331. [[CrossRef](#)]
35. Vieillard, J.; Bouazizi, N.; Bargougui, R.; Brun, N.; Nkuigue, P.F.; Oliviero, E.; Thoumire, O.; Couvrat, N.; Woumfo, E.D.; Ladam, G.; et al. Cocoa shell-deriving hydrochar modified through aminosilane grafting and cobalt particle dispersion as potential carbon dioxide adsorbent. *Chem. Eng. J.* **2018**, *342*, 420–428. [[CrossRef](#)]
36. Unnithan, M.R.; Vinod, V.P.; Anirudhan, T.S. Synthesis, Characterization, and Application as a Chromium(VI) Adsorbent of Amine-Modified Polyacrylamide-Grafted Coconut Coir Pith. *Ind. Eng. Chem. Res.* **2004**, *43*, 2247–2255. [[CrossRef](#)]
37. Anirudhan, T.S.; Rijith, S.; Divya, L. Preparation and Application of a Novel Functionalized Coconut Coir Pith as a Recyclable Adsorbent for Phosphate Removal. *Sep. Sci. Technol.* **2009**, *44*, 2774–2796. [[CrossRef](#)]
38. Tang, Y.; Liang, S.; Yu, S.; Gao, N.; Zhang, J.; Guo, H.; Wang, Y. Enhanced adsorption of humic acid on amine functionalized magnetic mesoporous composite microspheres. *Colloids Surf. A Physicochem. Eng. Asp.* **2012**, *406*, 61–67. [[CrossRef](#)]
39. Jin, S.; Park, B.C.; Ham, W.S.; Pan, L.; Kim, Y.K. Effect of the magnetic core size of amino-functionalized Fe₃O₄-mesoporous SiO₂ core-shell nanoparticles on the removal of heavy metal ions. *Colloids Surf. A Physicochem. Eng. Asp.* **2017**, *531*, 133–140. [[CrossRef](#)]
40. El-Dessouky, M.I.; Ibrahem, H.H.; El-Masry, E.H.; El-Deen, G.E.S.; Sami, N.M.; Moustafa, M.E.; Mabrouk, E.M. Removal of Cs⁺ and Co²⁺ ions from aqueous solutions using poly (acrylamide-acrylic acid)/kaolin composite prepared by gamma radiation. *Appl. Clay Sci.* **2018**, *151*, 73–80. [[CrossRef](#)]
41. Gardi, I.; Mishael, Y.G. Designing a regenerable stimuli-responsive grafted polymer-clay sorbent for filtration of water pollutants. *Sci. Technol. Adv. Mater.* **2018**, *19*, 588–598. [[CrossRef](#)]
42. Lozano-Morales, V.; Gardi, I.; Nir, S.; Undabeytia, T. Removal of pharmaceuticals from water by clay-cationic starch sorbents. *J. Clean. Prod.* **2018**, *190*, 703–711. [[CrossRef](#)]
43. Kohay, H.; Izbitski, A.; Mishael, Y.G. Developing Polycation-Clay Sorbents for Efficient Filtration of Diclofenac: Effect of Dissolved Organic Matter and Comparison to Activated Carbon. *Environ. Sci. Technol.* **2015**, *49*, 9280–9288. [[CrossRef](#)] [[PubMed](#)]
44. Cho, D.-W.; Jeon, B.-H.; Chon, C.-M.; Kim, Y.; Schwartz, F.W.; Lee, E.-S.; Song, H. A novel chitosan/clay/magnetite composite for adsorption of Cu(II) and As(V). *Chem. Eng. J.* **2012**, *200–202*, 654–662. [[CrossRef](#)]
45. Koushkgah, S.; Zakialamdar, A.; Pishnamazi, M.; Ramandi, H.F.; Aliabadi, M.; Irani, M. Aminated-Fe₃O₄ nanoparticles filled chitosan/PVA/PES dual layers nanofibrous membrane for the removal of Cr(VI) and Pb(II) ions from aqueous solutions in adsorption and membrane processes. *Chem. Eng. J.* **2018**, *337*, 169–182. [[CrossRef](#)]
46. Guo, X.; Du, B.; Wei, Q.; Yang, J.; Hu, L.; Yan, L.-G.; Xu, W. Synthesis of amino functionalized magnetic graphenes composite material and its application to remove Cr(VI), Pb(II), Hg(II), Cd(II) and Ni(II) from contaminated water. *J. Hazard. Mater.* **2014**, *278*, 211–220. [[CrossRef](#)]

47. Baghani, A.N.; Mahvi, A.H.; Gholami, M.; Rastkari, N.; Delikhoon, M. One-Pot synthesis, characterization and adsorption studies of amine-functionalized magnetite nanoparticles for removal of Cr (VI) and Ni (II) ions from aqueous solution: Kinetic, isotherm and thermodynamic studies. *J. Environ. Health Sci. Eng.* **2016**, *14*, 11. [[CrossRef](#)]
48. Nonkumwong, J.; Ananta, S.; Srisombat, L. Effective removal of lead(ii) from wastewater by amine-functionalized magnesium ferrite nanoparticles. *RSC Adv.* **2016**, *6*, 47382–47393. [[CrossRef](#)]
49. Zendehdel, M.; Ramezani, M.; Shoshtari-Yeganeh, B.; Cruciani, G.; Salmani, A. Simultaneous removal of Pb(II), Cd(II) and bacteria from aqueous solution using amino-functionalized $\text{Fe}_3\text{O}_4/\text{NaP}$ zeolite nanocomposite. *Environ. Technol.* **2019**, *40*, 3689–3704. [[CrossRef](#)]
50. Li, Z.; Pan, Z.; Wang, Y. Preparation of ternary amino-functionalized magnetic nano-sized illite-smectite clay for adsorption of Pb(II) ions in aqueous solution. *Environ. Sci. Pollut. Res.* **2020**, *27*, 11683–11696. [[CrossRef](#)] [[PubMed](#)]
51. Morsi, R.E.; Al-Sabagh, A.M.; Moustafa, Y.M.; ElKholy, S.G.; Sayed, M.S. Polythiophene modified chitosan/magnetite nanocomposites for heavy metals and selective mercury removal. *Egypt. J. Pet.* **2018**, *27*, 1077–1085. [[CrossRef](#)]
52. Hao, H.; Liu, G.; Wang, Y.; Shi, B.; Han, K.; Zhuang, Y.; Kong, Y. Simultaneous cationic Cu (II)-anionic Sb (III) removal by $\text{NH}_2\text{-Fe}_3\text{O}_4\text{-NTA}$ core-shell magnetic nanoparticle sorbents synthesized via a facile one-pot approach. *J. Hazard. Mater.* **2019**, *362*, 246–257. [[CrossRef](#)]
53. Hamza, M.F.; Wei, Y.; Mira, H.; Abdel-Rahman, A.A.-H.; Guibal, E. Synthesis and adsorption characteristics of grafted hydrazinyl amine magnetite-chitosan for Ni(II) and Pb(II) recovery. *Chem. Eng. J.* **2019**, *362*, 310–324. [[CrossRef](#)]
54. Feitoza, N.C.; Gonçalves, T.D.; Mesquita, J.J.; Menegucci, J.S.; Santos, M.-K.M.; Chaker, J.A.; Cunha, R.B.; Medeiros, A.; Rubim, J.C.; Sousa, M.H. Fabrication of glycine-functionalized maghemite nanoparticles for magnetic removal of copper from wastewater. *J. Hazard. Mater.* **2014**, *264*, 153–160. [[CrossRef](#)]
55. Wei, W.; Desiraju, H.K.R.; Bediako, J.K.; Yun, Y.-S. Aliquat-336-impregnated alginate capsule as a green sorbent for selective recovery of gold from metal mixtures. *Chem. Eng. J.* **2016**, *289*, 413–422. [[CrossRef](#)]
56. Bao, S.; Tang, L.; Li, K.; Ning, P.; Peng, J.; Guo, H.; Zhu, T.; Liu, Y. Highly selective removal of Zn(II) ion from hot-dip galvanizing pickling waste with amino-functionalized $\text{Fe}_3\text{O}_4@\text{SiO}_2$ magnetic nano-adsorbent. *J. Colloid Interface Sci.* **2016**, *462*, 235–242. [[CrossRef](#)]
57. Zhou, G.; Wang, Y.; Zhou, R.; Wang, C.; Jin, Y.; Qiu, J.; Hua, C.; Cao, Y. Synthesis of amino-functionalized bentonite/ $\text{CoFe}_3\text{O}_4@\text{MnO}_2$ magnetic recoverable nanoparticles for aqueous Cd^{2+} removal. *Sci. Total Environ.* **2019**, *682*, 505–513. [[CrossRef](#)] [[PubMed](#)]
58. Saleh, T.A.; Adio, S.O.; Asif, M.; Dafalla, H. Statistical analysis of phenols adsorption on diethylenetriamine-modified activated carbon. *J. Clean. Prod.* **2018**, *182*, 960–968. [[CrossRef](#)]
59. Peng, X.; Hu, F.; Zhang, T.; Qiu, F.; Dai, H. Amine-functionalized magnetic bamboo-based activated carbon adsorptive removal of ciprofloxacin and norfloxacin: A batch and fixed-bed column study. *Bioresour. Technol.* **2018**, *249*, 924–934. [[CrossRef](#)] [[PubMed](#)]
60. Morshed, M.N.; Bouazizi, N.; Behary, N.; Vieillard, J.; Thoumire, O.; Nierstrasz, V.; Azzouz, A. Iron-loaded amine/thiol functionalized polyester fibers with high catalytic activities: A comparative study. *Dalton Trans.* **2019**, *48*, 8384–8399. [[CrossRef](#)]
61. Iannicelli-Zubiani, E.M.; Stampino, P.G.; Cristiani, C.; Dotelli, G. Enhanced lanthanum adsorption by amine modified activated carbon. *Chem. Eng. J.* **2018**, *341*, 75–82. [[CrossRef](#)]
62. Mathew, A.; Parambadath, S.; Barnabas, M.J.; Song, H.J.; Kim, J.-S.; Park, S.S.; Ha, C.-S. Rhodamine 6G assisted adsorption of metanil yellow over succinamic acid functionalized MCM-41. *Dye. Pigment.* **2016**, *131*, 177–185. [[CrossRef](#)]
63. Wu, P.; Dai, Y.; Long, H.; Zhu, N.; Li, P.; Wu, J.; Dang, Z. Characterization of organo-montmorillonites and comparison for Sr(II) removal: Equilibrium and kinetic studies. *Chem. Eng. J.* **2012**, *191*, 288–296. [[CrossRef](#)]
64. Bauer, F.; Czihal, S.; Bertmer, M.; Decker, U.; Naumov, S.; Wassersleben, S.; Enke, D. Water-based functionalization of mesoporous siliceous materials, Part 1: Morphology and stability of grafted 3-aminopropyltriethoxysilane. *Microporous Mesoporous Mater.* **2017**, *250*, 221–231. [[CrossRef](#)]
65. Xue, A.; Zhou, S.; Zhao, Y.; Lu, X.; Han, P. Effective NH₂-grafting on attapulgite surfaces for adsorption of reactive dyes. *J. Hazard. Mater.* **2011**, *194*, 7–14. [[CrossRef](#)] [[PubMed](#)]
66. Monasterio, M.; Gaitero, J.J.; Erkizia, E.; Bustos, A.G.; Miccio, L.A.; Dolado, J.S.; Cerveny, S. Effect of addition of silica- and amine functionalized silica-nanoparticles on the microstructure of calcium silicate hydrate (C-S-H) gel. *J. Colloid Interface Sci.* **2015**, *450*, 109–118. [[CrossRef](#)]
67. Shen, W.; He, H.; Zhu, J.; Yuan, P.; Ma, Y.; Liang, X. Preparation and characterization of 3-aminopropyltriethoxysilane grafted montmorillonite and acid-activated montmorillonite. *Sci. Bull.* **2009**, *54*, 265–271. [[CrossRef](#)]
68. Demirbaş, Ö.; Alkan, M.; Doğan, M.; Turhan, Y.; Namli, H.; Turan, P. Electrokinetic and adsorption properties of sepiolite modified by 3-aminopropyltriethoxysilane. *J. Hazard. Mater.* **2007**, *149*, 650–656. [[CrossRef](#)]
69. Ozmen, M.; Can, K.; Arslan, G.; Tor, A.; Cengeloglu, Y.; Ersoz, M. Adsorption of Cu(II) from aqueous solution by using modified Fe_3O_4 magnetic nanoparticles. *Desalination* **2010**, *254*, 162–169. [[CrossRef](#)]
70. Tao, Q.; Fang, Y.; Li, T.; Zhang, D.; Chen, M.; Ji, S.; He, H.; Komarneni, S.; Zhang, H.; Dong, Y.; et al. Silylation of saponite with 3-aminopropyltriethoxysilane. *Appl. Clay Sci.* **2016**, *132–133*, 133–139. [[CrossRef](#)]
71. Xiong, C.; Wang, S.; Sun, W.; Li, Y. Selective adsorption of Pb(II) from aqueous solution using nanosilica functionalized with diethanolamine: Equilibrium, kinetic and thermodynamic. *Microchem. J.* **2019**, *146*, 270–278. [[CrossRef](#)]
72. Xiong, Y.; Cui, X.; Wang, D.; Wang, Y.; Lou, Z.; Shan, W.; Fan, Y. Diethanolamine functionalized rice husk for highly efficient recovery of gallium(III) from solution and a mechanism study. *Mater. Sci. Eng. C* **2019**, *99*, 1115–1122. [[CrossRef](#)]

73. Javadian, H.; Koutenaei, B.B.; Shekarian, E.; Sorkhrodi, F.Z.; Khatti, R.; Toosi, M. Application of functionalized nano HMS type mesoporous silica with N-(2-aminoethyl)-3-aminopropyl methyldimethoxysilane as a suitable adsorbent for removal of Pb (II) from aqueous media and industrial wastewater. *J. Saudi Chem. Soc.* **2017**, *21*, S219–S230. [[CrossRef](#)]
74. Bouazizi, N.; Khelil, M.; Ajala, F.; Boudharaa, T.; Benghnia, A.; Lachheb, H.; Ben Slama, R.; Chaouachi, B.; M’Nif, A.; Azzouz, A. Molybdenum-loaded 1,5-diaminonaphthalene/ZnO materials with improved electrical properties and affinity towards hydrogen at ambient conditions. *Int. J. Hydrogen Energy* **2016**, *41*, 11232–11241. [[CrossRef](#)]
75. Anyanwu, J.-T.; Wang, Y.; Yang, R.T. Influence of water on amine loading for ordered mesoporous silica. *Chem. Eng. Sci.* **2021**, *241*, 116717. [[CrossRef](#)]
76. Gao, P.; Chen, D.; Chen, W.; Sun, J.; Wang, G.; Zhou, L. Facile synthesis of amine-crosslinked starch as an efficient biosorbent for adsorptive removal of anionic organic pollutants from water. *Int. J. Biol. Macromol.* **2021**, *191*, 1240–1248. [[CrossRef](#)]
77. Zha, Q.; Sang, X.; Liu, D.; Wang, D.; Shi, G.; Ni, C. Modification of hydrophilic amine-functionalized metal-organic frameworks to hydrophobic for dye adsorption. *J. Solid State Chem.* **2019**, *275*, 23–29. [[CrossRef](#)]
78. Ahmad, N.; Nordin, N.A.H.M.; Jaafar, J.; Malek, N.A.N.N.; Ismail, A.F.; Ramli, M.K.N. Modification of zeolitic imidazolate framework-8 with amine groups for improved antibacterial activity. *Mater. Today Proc.* **2021**, *46*, 2024–2029. [[CrossRef](#)]
79. Xue, A.; Zhou, S.; Zhao, Y.; Lu, X.; Han, P. Adsorption of reactive dyes from aqueous solution by silylated palygorskite. *Appl. Clay Sci.* **2010**, *48*, 638–640. [[CrossRef](#)]
80. Bertuoli, P.T.; Piazza, D.; Scienza, L.C.; Zattera, A.J. Preparation and characterization of montmorillonite modified with 3-aminopropyltriethoxysilane. *Appl. Clay Sci.* **2014**, *87*, 46–51. [[CrossRef](#)]
81. Yang, S.-Q.; Yuan, P.; He, H.-P.; Qin, Z.-H.; Zhou, Q.; Zhu, J.; Liu, D. Effect of reaction temperature on grafting of γ -aminopropyl triethoxysilane (APTES) onto kaolinite. *Appl. Clay Sci.* **2012**, *62–63*, 8–14. [[CrossRef](#)]
82. Zhang, W.; Li, Y.; Li, Y.; Gao, E.; Cao, G.; Bernards, M.T.; He, Y.; Shi, Y. Enhanced SO₂ Resistance of Tetraethylenepentammonium Nitrate Protic Ionic Liquid-Functionalized SBA-15 during CO₂ Capture from Flue Gas. *Energy Fuels* **2020**, *34*, 8628–8634. [[CrossRef](#)]
83. Choi, W.; Min, K.; Kim, C.; Ko, Y.S.; Jeon, J.W.; Seo, H.; Park, Y.-K.; Choi, M. Epoxide-functionalization of polyethyleneimine for synthesis of stable carbon dioxide adsorbent in temperature swing adsorption. *Nat. Commun.* **2016**, *7*, 12640. [[CrossRef](#)] [[PubMed](#)]
84. Park, S.; Choi, K.; Yu, H.J.; Won, Y.-J.; Kim, C.; Choi, M.; Cho, S.-H.; Lee, J.-H.; Lee, S.Y.; Lee, J.S. Thermal Stability Enhanced Tetraethylenepentamine/Silica Adsorbents for High Performance CO₂ Capture. *Ind. Eng. Chem. Res.* **2018**, *57*, 4632–4639. [[CrossRef](#)]
85. Takeuchi, M.; Martra, G.; Coluccia, S.; Anpo, M. Investigations of the Structure of H₂O Clusters Adsorbed on TiO₂ Surfaces by Near-Infrared Absorption Spectroscopy. *J. Phys. Chem. B* **2005**, *109*, 7387–7391. [[CrossRef](#)] [[PubMed](#)]
86. Morterra, C. An infrared spectroscopic study of anatase properties. Part 6.—Surface hydration and strong Lewis acidity of pure and sulphate-doped preparations. *J. Chem. Soc. Faraday Trans. 1 Phys. Chem. Condens. Phases* **1988**, *84*, 1617–1637. [[CrossRef](#)]
87. Paul, G.; Musso, G.E.; Bottinelli, E.; Cossi, M.; Marchese, L.; Berlier, G. Investigating the Interaction of Water Vapour with Aminopropyl Groups on the Surface of Mesoporous Silica Nanoparticles. *ChemPhysChem* **2017**, *18*, 839–849. [[CrossRef](#)]
88. Iliade, P.; Miletto, I.; Coluccia, S.; Berlier, G. Functionalization of mesoporous MCM-41 with aminopropyl groups by co-condensation and grafting: A physico-chemical characterization. *Res. Chem. Intermed.* **2012**, *38*, 785–794. [[CrossRef](#)]
89. Zhang, L.; Liu, J.; Yang, J.; Yang, Q.; Li, C. Direct synthesis of highly ordered amine-functionalized mesoporous ethane-silicas. *Microporous Mesoporous Mater.* **2008**, *109*, 172–183. [[CrossRef](#)]
90. Calvo, A.; Angelomé, P.; Sánchez, V.M.; Scherlis, D.A.; Williams, F.; Soler-Illia, G. Mesoporous Aminopropyl-Functionalized Hybrid Thin Films with Modulable Surface and Environment-Responsive Behavior. *Chem. Mater.* **2008**, *20*, 4661–4668. [[CrossRef](#)]
91. Chiang, C.-H.; Ishida, H.; Koenig, J.L. The structure of γ -aminopropyltriethoxysilane on glass surfaces. *J. Colloid Interface Sci.* **1980**, *74*, 396–404. [[CrossRef](#)]
92. Gys, N.; Siemons, L.; Pawlak, B.; Wyns, K.; Baert, K.; Hauffman, T.; Adriaensens, P.; Blockhuys, F.; Michielsen, B.; Mullens, S.; et al. Experimental and computational insights into the aminopropylphosphonic acid modification of mesoporous TiO₂ powder: The role of the amine functionality on the surface interaction and coordination. *Appl. Surf. Sci.* **2021**, *566*, 150625. [[CrossRef](#)]
93. Wielant, J.; Hauffman, T.; Blajiev, O.; Hausbrand, R.; Terryn, H. Influence of the Iron Oxide Acid–Base Properties on the Chemisorption of Model Epoxy Compounds Studied by XPS. *J. Phys. Chem. C* **2007**, *111*, 13177–13184. [[CrossRef](#)]
94. Gadois, C.; Świątowska, J.; Zanna, S.; Marcus, P. Influence of Titanium Surface Treatment on Adsorption of Primary Amines. *J. Phys. Chem. C* **2013**, *117*, 1297–1307. [[CrossRef](#)]
95. Abrahami, S.; Hauffman, T.; De Kok, J.M.; Mol, A.; Terryn, H. XPS Analysis of the Surface Chemistry and Interfacial Bonding of Barrier-Type Cr(VI)-Free Anodic Oxides. *J. Phys. Chem. C* **2015**, *119*, 19967–19975. [[CrossRef](#)]
96. Bovone, G.; Dudaryeva, O.Y.; Marco-Dufort, B.; Tibbitt, M.W. Engineering Hydrogel Adhesion for Biomedical Applications via Chemical Design of the Junction. *ACS Biomater. Sci. Eng.* **2021**, *7*, 4048–4076. [[CrossRef](#)] [[PubMed](#)]
97. Rose, S.; Prevotet, A.; Elzière, P.; Hourdet, D.; Marcellan, A.; Leibler, L. Nanoparticle solutions as adhesives for gels and biological tissues. *Nature* **2014**, *505*, 382–385. [[CrossRef](#)]
98. Azzouz, A.; Nousir, S.; Bouazizi, N.; Roy, R. Metal-Inorganic-Organic Matrices as Efficient Sorbents for Hydrogen Storage. *ChemSusChem* **2015**, *8*, 800–803. [[CrossRef](#)] [[PubMed](#)]

99. Khan, Z.U.H.; Khan, A.; Shah, A.; Wan, P.; Chen, Y.; Khan, G.M.; Khan, A.U.; Tahir, K.; Muhammad, N.; Khan, H.U. Enhanced photocatalytic and electrocatalytic applications of green synthesized silver nanoparticles. *J. Mol. Liq.* **2016**, *220*, 248–257. [[CrossRef](#)]
100. Nasrollahzadeha, M.; Baran, T.; Baran, N.Y.; Sajjadia, M.; Tahsili, M.R.; Shokouhimehre, M. Pd nanocatalyst stabilized on amine-modified zeolite: Antibacterial and catalytic activities for environmental pollution remediation in aqueous medium. *Sep. Purif. Technol.* **2020**, *239*, 116542. [[CrossRef](#)]
101. Liu, W.; Yang, Q.; Yang, Z.; Wang, W. Adsorption of 2,4-D on magnetic graphene and mechanism study. *Colloids Surfaces A Physicochem. Eng. Asp.* **2016**, *509*, 367–375. [[CrossRef](#)]
102. Liu, Y.; Zhang, X.; Wang, J. A critical review of various adsorbents for selective removal of nitrate from water: Structure, performance and mechanism. *Chemosphere* **2021**, *291*, 132728. [[CrossRef](#)] [[PubMed](#)]
103. Bakhta, S.; Sadaoui, Z.; Lassi, U.; Romar, H.; Kupila, R.; Vieillard, J. Performances of metals modified activated carbons for fluoride removal from aqueous solutions. *Chem. Phys. Lett.* **2020**, *754*, 137705. [[CrossRef](#)]
104. Fotsing, P.N.; Woumfo, E.D.; Mezghich, S.; Mignot, M.; Mofaddel, N.; Le Derf, F.; Vieillard, J. Surface modification of biomaterials based on cocoa shell with improved nitrate and Cr(vi) removal. *RSC Adv.* **2020**, *10*, 20009–20019. [[CrossRef](#)]
105. Dindar, M.H.; Yaftian, M.R.; Rostamnia, S. Potential of functionalized SBA-15 mesoporous materials for decontamination of water solutions from Cr(VI), As(V) and Hg(II) ions. *J. Environ. Chem. Eng.* **2015**, *3*, 986–995. [[CrossRef](#)]
106. Guerra, D.; Mello, I.; Resende, R.; Silva, R. Application as adsorbents of natural and functionalized Brazilian bentonite in Pb²⁺ adsorption: Equilibrium, kinetic, pH, and thermodynamic effects. *Water Resour. Ind.* **2013**, *4*, 32–50. [[CrossRef](#)]
107. Marjanovic, V.; Lazarevic, S.; Jankovic-Castvan, I.; Jokic, B.; Bjelajac, A.; Janackovic, D.; Petrovic, R. Functionalization of thermo-acid activated sepiolite by amine-silane and mercapto-silane for chromium(VI) adsorption from aqueous solutions. *Chem. Ind.* **2013**, *67*, 715–728. [[CrossRef](#)]
108. Keshvardoostchokami, M.; Majidi, M.; Zamani, A.; Liu, B. A review on the use of chitosan and chitosan derivatives as the bio-adsorbents for the water treatment: Removal of nitrogen-containing pollutants. *Carbohydr. Polym.* **2021**, *273*, 118625. [[CrossRef](#)]
109. Gao, Y.; Ru, Y.; Zhou, L.; Wang, X.; Wang, J. Preparation and characterization of chitosan-zeolite molecular sieve composite for ammonia and nitrate removal. *Compos. Adv. Mater.* **2018**, *27*, 185–192. [[CrossRef](#)]
110. Lou, Z.; Zhang, W.; Hu, X.; Zhang, H. Synthesis of a novel functional group-bridged magnetized bentonite adsorbent: Characterization, kinetics, isotherm, thermodynamics and regeneration. *Chin. J. Chem. Eng.* **2017**, *25*, 587–594. [[CrossRef](#)]
111. Araghi, S.H.; Entezari, M.H.; Chamsaz, M. Modification of mesoporous silica magnetite nanoparticles by 3-aminopropyltriethoxysilane for the removal of Cr(VI) from aqueous solution. *Microporous Mesoporous Mater.* **2015**, *218*, 101–111. [[CrossRef](#)]
112. Morshed, M.N.; Bouazizi, N.; Behary, N.; Guan, J.; Nierstrasz, V. Stabilization of zero valent iron (Fe⁰) on plasma/dendrimer functionalized polyester fabrics for Fenton-like removal of hazardous water pollutants. *Chem. Eng. J.* **2019**, *374*, 658–673. [[CrossRef](#)]
113. Laaz, I.; Stébé, M.-J.; Benhamou, A.; Zoubir, D.; Blin, J.-L. Influence of porosity and surface modification on the adsorption of both cationic and anionic dyes. *Colloids Surf. A Physicochem. Eng. Asp.* **2016**, *490*, 30–40. [[CrossRef](#)]
114. Dutta, S.; Gupta, B.; Srivastava, S.K.; Gupta, A.K. Recent advances on the removal of dyes from wastewater using various adsorbents: A critical review. *Mater. Adv.* **2021**, *2*, 4497–4531. [[CrossRef](#)]
115. Gupta, V.K.; Jain, R.; Mittal, D.A.; Saleh, T.; Nayak, A.; Agarwal, S.; Sikarwar, S. Photo-catalytic degradation of toxic dye amaranth on TiO₂/UV in aqueous suspensions. *Mater. Sci. Eng. C* **2012**, *32*, 12–17. [[CrossRef](#)] [[PubMed](#)]
116. Saleh, T.; Gupta, V.K. Column with CNT/magnesium oxide composite for lead(II) removal from water. *Environ. Sci. Pollut. Res.* **2012**, *19*, 1224–1228. [[CrossRef](#)]
117. Gupta, V.; Srivastava, S.; Mohan, D.; Sharma, S. Design parameters for fixed bed reactors of activated carbon developed from fertilizer waste for the removal of some heavy metal ions. *Waste Manag.* **1998**, *17*, 517–522. [[CrossRef](#)]
118. Mittal, A.; Mittal, J.; Malviya, A.; Kaur, D.; Gupta, V. Decoloration treatment of a hazardous triaryl methane dye, Light Green SF (Yellowish) by waste material adsorbents. *J. Colloid Interface Sci.* **2010**, *342*, 518–527. [[CrossRef](#)]
119. Song, H.; Rioux, R.M.; Hoefelmeyer, J.; Komor, R.; Niesz, K.; Grass, M.; Yang, A.P.; Somorjai, G.A. Hydrothermal Growth of Mesoporous SBA-15 Silica in the Presence of PVP-Stabilized Pt Nanoparticles: Synthesis, Characterization, and Catalytic Properties. *J. Am. Chem. Soc.* **2006**, *128*, 3027–3037. [[CrossRef](#)]
120. Panigrahi, S.; Basu, S.; Praharaj, S.; Pande, S.; Jana, S.; Pal, A.; Ghosh, S.K.; Pal, T. Synthesis and Size-Selective Catalysis by Supported Gold Nanoparticles: Study on Heterogeneous and Homogeneous Catalytic Process. *J. Phys. Chem. C* **2007**, *111*, 4596–4605. [[CrossRef](#)]
121. Lu, H.; Yu, L.; Liu, Q.; Du, J. Ultrafine silver nanoparticles with excellent antibacterial efficacy prepared by a handover of vesicle templating to micelle stabilization. *Polym. Chem.* **2013**, *4*, 3448–3452. [[CrossRef](#)]
122. Aditya, T.; Pal, A.; Pal, T. Nitroarene reduction: A trusted model reaction to test nanoparticle catalysts. *Chem. Commun.* **2015**, *51*, 9410–9431. [[CrossRef](#)]
123. Bae, S.; Gim, S.; Kim, H.; Hanna, K. Effect of NaBH 4 on properties of nanoscale zero-valent iron and its catalytic activity for reduction of p-nitrophenol. *Appl. Catal. B Environ.* **2016**, *182*, 541–549. [[CrossRef](#)]
124. Zhang, Z.; Huang, H.; Yang, X.; Zang, L. Tailoring Electronic Properties of Graphene by π–π Stacking with Aromatic Molecules. *J. Phys. Chem. Lett.* **2011**, *2*, 2897–2905. [[CrossRef](#)]

125. Viswanathan, B.; Tanaka, K.; Toyoshima, I. Cluster model and charge transfer in a strong metal-support interaction (SMSI) state. *Langmuir* **1986**, *2*, 113–116. [[CrossRef](#)]
126. Alighardashi, A.; Esfahani, Z.K.; Afkhami, A.; Najafi, F.; Hassan, N. Comparison of the efficiency of graphene oxide, activated graphene oxide, dendrimer-graphene oxide and activated dendrimer-graphene oxide for nitrate removal from aqueous solutions. *Desalination Water Treat.* **2017**, *100*, 100–115. [[CrossRef](#)]
127. Yazdi, F.; Anbia, M.; Salehi, S. Characterization of functionalized chitosan-clinoptilolite nanocomposites for nitrate removal from aqueous media. *Int. J. Biol. Macromol.* **2019**, *130*, 545–555. [[CrossRef](#)] [[PubMed](#)]
128. Ryu, S.C.; Kim, J.Y.; Hwang, M.J.; Moon, H. Recovery of nitrate from water streams using amine-grafted and magnetized SBA-15. *Korean J. Chem. Eng.* **2018**, *35*, 489–497. [[CrossRef](#)]
129. Wu, Y.; Wang, Y.; Wang, J.; Xu, S.; Yu, L.; Philippe, C.; Wintgens, T. Nitrate removal from water by new polymeric adsorbent modified with amino and quaternary ammonium groups: Batch and column adsorption study. *J. Taiwan Inst. Chem. Eng.* **2016**, *66*, 191–199. [[CrossRef](#)]
130. Kheshti, Z.; Hassanajili, S. Novel Multifunctional Mesoporous Microsphere with High Surface Area for Removal of Zinc Ion from Aqueous Solution: Preparation and Characterization. *J. Inorg. Organomet. Polym. Mater.* **2017**, *27*, 1613–1626. [[CrossRef](#)]
131. Aguado, S.; Quirós, J.; Canivet, J.; Farrusseng, D.; Boltes, K.; Rosal, R. Antimicrobial activity of cobalt imidazolate metal–organic frameworks. *Chemosphere* **2014**, *113*, 188–192. [[CrossRef](#)]
132. Zardini, H.Z.; Amiri, A.; Shanbedi, M.; Maghrebi, M.; Baniadam, M. Enhanced antibacterial activity of amino acids-functionalized multi walled carbon nanotubes by a simple method. *Colloids Surf. B Biointerfaces* **2012**, *92*, 196–202. [[CrossRef](#)] [[PubMed](#)]
133. Hanim, S.A.M.; Malek, N.A.N.N.; Ibrahim, Z. Amine-functionalized, silver-exchanged zeolite NaY: Preparation, characterization and antibacterial activity. *Appl. Surf. Sci.* **2016**, *360*, 121–130. [[CrossRef](#)]
134. Furchtgott, L.; Wingreen, N.S.; Huang, K.C. Mechanisms for maintaining cell shape in rod-shaped Gram-negative bacteria. *Mol. Microbiol.* **2011**, *81*, 340–353. [[CrossRef](#)] [[PubMed](#)]
135. Kwakye-Awuah, B.; Williams, C.; Kenward, M.; Radecka, I. Antimicrobial action and efficiency of silver-loaded zeolite X. *J. Appl. Microbiol.* **2008**, *104*, 1516–1524. [[CrossRef](#)] [[PubMed](#)]
136. Jung, W.K.; Koo, H.C.; Kim, K.W.; Shin, S.; Kim, S.H.; Park, Y.H. Antibacterial Activity and Mechanism of Action of the Silver Ion in *Staphylococcus aureus* and *Escherichia coli*. *Appl. Environ. Microbiol.* **2008**, *74*, 2171–2178. [[CrossRef](#)] [[PubMed](#)]